Bioresource Technology

Particle Swarm Optimization and Global Sensitivity Analysis for Catalytic Co-Pyrolysis of Chlorella vulgaris and Plastic Waste Mixtures

--Manuscript Draft--

Manuscript Number:	BITE-D-20-08864R2
Article Type:	Original research paper
Keywords:	Co-pyrolysis; Microalgae Chlorella vulgaris; High-Density Polyethylene Waste; Kinetics; Particle Swarm Optimization; Thermodynamic
Corresponding Author:	Bridgid Lai Fui Chin, PhD Curtin University Malaysia Miri, MALAYSIA
First Author:	Mahrima Majid, Bachelor of Chemical Engineering
Order of Authors:	Mahrima Majid, Bachelor of Chemical Engineering
	Bridgid Lai Fui Chin, PhD
	Zeinab Abbas Jawad, PhD in Chemical Engineering
	Yee Ho Chai, phD in Chemical Engineering
	Man Kee Lam, phD in Chemical Engineering
	Suzana Yusup, phD in Chemical Engineering
	Kin Wai Cheah, PhD in Chemical Engineering
Abstract:	This study investigated on the co-pyrolysis of microalgae Chlorella vulgaris and high-density polyethylene (HDPE) waste mixtures which was performed with three types of catalysts, namely limestone (LS), HZSM-5 zeolite, and novel bi-functional LS/HZSM-5/LS. Kissinger-Kai (K-K) model-free method was coupled with Particle Swarm Optimization (PSO) model-fitting method using the thermogravimetric experimental data. A global sensitivity analysis was carried out using Latin Hypercube Sampling and rank transformation to assess the extent of impact of the input kinetic parameters on the output results. Furthermore, a thermodynamic analysis was performed to obtain parameters such as enthalpy change (ΔH), Gibb's free energy (ΔG), and entropy change (ΔS). The activation energy (EA) of the microalgae Chlorella vulgaris and HDPE binary mixture were found to be lower upon the addition of catalysts. Among the catalyst used, bi-functional LS/HZSM-5 catalyst exhibited the lowest EA (83.59 kJ/mol) and ∆H (78 kJ/mol) as compared to LS and HZSM-5 catalysts.

Curtin University
Sarawak Malaysia

CDT 250, 98009 Miri
Sarawak, Malaysia

Telephone +60 85 443939
Facsimile +60 85 443838
Email enquiries@curtin.edu.my
Web www.curtin.edu.my

27th December 2020

Prof. Ashok Pandey
Editor-in-Chief
ELSEVIER Bioresource Technology

Subject: Submission of an article for publication in ELSEVIER Bioresource Technology

Dear Editor-in-Chief,

On behalf of my co-authors and myself, I am submitting the enclosed article entitled **'Particle Swarm Optimization and Global Sensitivity Analysis for Catalytic Co-Pyrolysis of Microalgae *Chlorella vulgaris* and Plastic Waste Mixtures: Thermal Degradation, Kinetic and Thermodynamic Parameters'**. The manuscript has not been submitted for publication nor has it been published before in whole or in part elsewhere. The other co-authors and I had agreed to submit this article to this journal.

The authors are in the opinion that the enclosed article fits well within the scope of ELSEVIER Renewable Energy i.e. **"Physico-Chemical & Thermo-Chemical Processes for Biomass (classification: 70.800 pyrolysis)"** that demonstrates the sustainable and renewable approach of thermochemical conversion specifically for catalytic co-pyrolysis of biomass microalgae *Chlorella vulgaris* and plastic waste i.e. high-density polyethylene utilizing different types of catalysts such as commercial HZSM-5 zeolite catalyst, natural limestone (LS) catalyst, and Bi-functional HZSM-5/LS catalysts for bioenergy production.

Many studies had reported extensively using lignocellulose biomass and has carried our using microalgae *Chlorella vulgaris* as a biomass. Nevertheless, many studies had also reviewed on the biomass conversion via catalytic pyrolysis process. However, there are still no kinetic and thermodynamic studies reported on comparing the non-catalytic and catalytic co-pyrolysis of microalgae *Chlorella vulgaris* and high polyethylene waste mixtures with the presence of catalyst for the bioenergy production. The main objectives of this paper is to conduct comparative studies of the kinetic and thermodynamic analysis of microalgae *Chlorella vulgaris* and high density polyethylene mixtures in pyrolysis process with and without the presence of commercial HZSM-5 zeolite catalyst, natural limestone (LS) catalyst, and Bi-functional HZSM-5/LS catalysts to further understand the catalytic pyrolysis mechanism in microalgae *Chlorella vulgaris* biomass and high density polyethylene. In this study, the Kissinger-Kai (K-K) model-free method was coupled with the Particle Swarm Optimization (PSO) model-fitting method using the thermogravimetric data. In addition, a global sensitivity analysis was carried out using Latin Hypercube Sampling and rank transformation to evaluate the impact of extend on the input kinetic parameters on the output results. Furthermore, thermodynamic analysis was also conducted to obtain enthalpy change (ΔH), Gibb's free energy (ΔG), and entropy change (ΔS). It was brought to attention that there is still a lacking of PSO and global sensitivity analyses on the catalytic co-pyrolysis of biomass and plastic waste mixtures.

The enclosed article investigates the kinetic and thermodynamic parameters of microalgae *Chlorella vulgaris* and high density polyethylene mixture with the presence of HZSM-5 zeolite catalyst, LS catalyst, and Bi-functional HZSM-5/LS catalyst via thermogravimetric approach (TGA). The K-K model free method was coupled with the PSO base optimization model-fitting using thermogravimetric experimental data in the range of heating rate studied i.e. 10-100 °C/min. It was found that the activation energy, E_A for the microalgae *Chlorella vulgaris* and HDPE waste mixtures was significantly reduced with the presence of bi-functional LS/HZSM-5 catalyst (83.59 kJ/mol as compared to LS catalyst (100.09 kJ/mol) and HZSM-5 catalyst (87.42 kJ/mol). This study evidently proven that Bi-functional HZSM-5/LS catalyst is a potential catalyst alternative for biomass and HDPE mixtures in co-pyrolysis processes. This work is carried out under the financial support from Ministry of High Education Malaysia through HICOE award to Centre of Biofuel and Biochemical Research (CBBR).

Selected Article Type: Submitted under "Original Article".

Yours sincerely,

Bridgid

Dr Bridgid Chin Lai Fui
Senior Lecturer
Department of Chemical Engineering
Faculty of Engineering and Science
Curtin University, Malaysia (Curtin Malaysia)
E-mail: bridgidchin@curtin.edu.my

Manuscript Ref. No.: **BITE-D-20-08864**

Title: **Particle Swarm Optimization and Global Sensitivity Analysis for Catalytic Co-Pyrolysis of Microalgae Chlorella vulgaris and Plastic Waste Mixtures: Thermal Degradation, Kinetic and Thermodynamic Parameters Study**

We thank the editor for the valuable comments that enabled us to enhance the quality of the manuscript. The following sections summarize our responses to all comments from the reviewers.

Editor:

No.	Comment	Action/Response
1.	Authors seem casual; have not followed GfA.	Thank you for your comment, editor. The manuscript had been revised to follow the GfA.
	Page length can be maximum 35 total.	The total page length is now 35 pages (manuscript = 24 pages, tables = 6 pages, and figures = 5 pages)
	Introduction is too long.	Thanks for your comment. The introduction length had been reduced.
	Refs can be maximum 50; delete some older ones.	The total number of reference is 44.

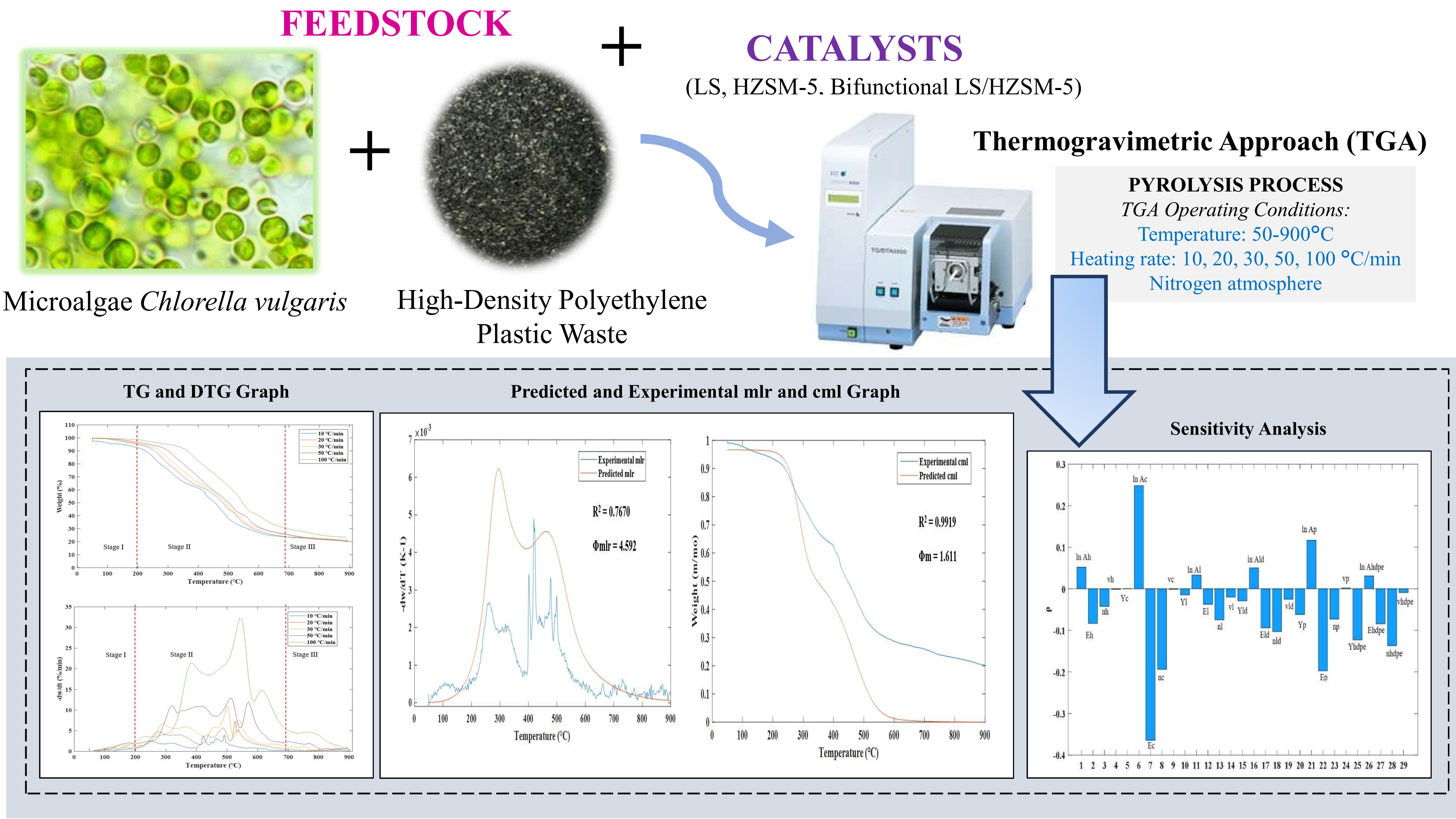
FEEDSTOCK
Microalgae Chlorella vulgaris
High-Density Polyethylene Plastic Waste
CATALYSTS
(LS, HZSM-5. Bifunctional LS/HZSM-5)
Thermogravimetric Approach (TGA)
PYROLYSIS PROCESS
TGA Operating Conditions:
Temperature: 50-900°C
Heating rate: 10, 20, 30, 50, 100 °C/min
Nitrogen atmosphere
TG and DTG Graph
Predicted and Experimental mlr and cml Graph
Sensitivity Analysis
Stage I
Stage II
Stage III
Temperature (°C)
Weight (%)
-dw/dt (%/min)
Experimental mlr
Predicted mlr
R² = 0.7670
Φmlr = 4.592
Experimental cml
Predicted cml
R² = 0.9919
Φm = 1.611
Weight (m/mo)
In Ac
In Ap
In Ald
In Al
In Ah
In Ahdpe
Ec
Ep
nc

Highlights

- Catalytic co-pyrolysis of microalgae and HDPE was investigated systematically.
- Lowest E_A (83.59 kJ/mol) was attained in the mixture using LS/HZSM-5 catalyst.
- Kissinger-Kai method was coupled with Particle Swarm Optimization (PSO).
- Implementation of global sensitivity analysis for kinetic analysis.
- Latin Hypercube Sampling and rank transformation were used.

Particle Swarm Optimization and Global Sensitivity Analysis for Catalytic Co-Pyrolysis of *Chlorella vulgaris* and Plastic Waste Mixtures

Mahrima Majid[a], Bridgid Lai Fui Chin[a*], Zeinab Abbas Jawad[b], Yee Ho Chai[c,d], Man Kee Lam[c,d], Suzana Yusup[c,d], Kin Wai Cheah[e,f]

[a]Department of Chemical Engineering, Faculty of Engineering and Science, Curtin University Malaysia, CDT 250, 98009 Miri Sarawak, Malaysia.

E-mail: (1) 700021403@student.curtin.edu.my (Mahrima Majid)

(2) bridgidchin@curtin.edu.my / bridgidchin@gmail.com (Dr Bridgid Lai Fui Chin)*

*Corresponding author

[b]Department of Chemical Engineering, College of Engineering, Qatar University, P.O. Box: 2713, Doha Qatar.

E-mail: zjawad@qu.edu.qa (Dr Zeinab Abbas Jawad)

[c]HiCoE-Centre for Biofuel and Biochemical Research, Institute of Self-Sustainable Building, Department of Chemical Engineering, Universiti Teknologi PETRONAS (UTP), Seri Iskandar 32610, Perak, Malaysia.

E-mail: (1) yeeho.chai@utp.edu.my (Dr Yee Ho Chai)

(2) lam.mankee@utp.edu.my (Dr Man Kee Lam)

(3) drsuzana_yusup@utp.edu.my (Prof Ir Suzana Yusup)

[d]Department of Chemical Engineering, Universiti Teknologi PETRONAS (UTP), 32610 Seri Iskandar, Perak, Malaysia.

[e]Energy and Environment Institute, University of Hull, Cottingham Road, Kingston upon Hull HU6 7RX, United Kingdom.

E-mail: K.Cheah@hull.ac.uk (Dr Kin Wai Cheah)

[f]B3 Challenge Group, Department of Chemical Engineering, University of Hull, Cottingham Road, Hull HU6 7RX, United Kingdom.

Keywords: Co-Pyrolysis, Microalgae *Chlorella vulgaris*, High-Density Polyethylene Waste, Kinetics, Particle Swarm Optimization, Thermodynamic

Abstract (149 words)

This study investigated on the co-pyrolysis of microalgae *Chlorella vulgaris* and high-density polyethylene (HDPE) waste mixtures which was performed with three types of catalysts, namely limestone (LS), HZSM-5 zeolite, and novel bi-functional LS/HZSM-5/LS. Kissinger-Kai (K-K) model-free method was coupled with Particle Swarm Optimization (PSO) model-fitting method using the thermogravimetric experimental data. A global sensitivity analysis was carried out using Latin Hypercube Sampling and rank transformation to assess the extent of impact of the input kinetic parameters on the output results. Furthermore, a thermodynamic analysis was performed to obtain parameters such as enthalpy change (ΔH), Gibb's free energy (ΔG), and entropy change (ΔS). The activation energy (E_A) of the microalgae *Chlorella vulgaris* and HDPE binary mixture were found to be lower upon the addition of catalysts. Among the catalyst used, bi-functional LS/HZSM-5 catalyst exhibited the lowest E_A (83.59 kJ/mol) and ΔH (78 kJ/mol) as compared to LS and HZSM-5 catalysts.

1.0 Introduction

In recent years, co-pyrolysis of biomass and plastic wastes has drawn a great attention within the scientist community in recent years due to its great potential to replace fossil fuel, resolve the world's ever-increasing municipal solid waste (MSW) problem (Ng et al. 2018), and can provide improvement to the quality and quantity of the bio-oil produced (Li et al. 2014b; Ryu et al. 2020). Pyrolysis of biomass alone have been reported to produce products with high oxygen and water content as well as high viscosity and corrosiveness all of which make the pyrolysis oil unsuitable to be used as fuel (Lam et al. 2019). Furthermore, biomass gives a low yield of aromatic compounds and high amount of coke as it contains a low hydrogen to carbon effective ratio, H/C_{eff} (Li et al. 2014b). Hence, the addition of plastics in the biomass pyrolysis could enhance the increased of H/C_{eff} (Ryu et al. 2019). The co-pyrolysis of biomass and plastic have also been reported to produce high quality bio-oil with increased calorific value. During co-pyrolysis, a positive coupling or synergistic effect exists due to an interaction between the biomass and plastic (Liew et al. 2021). The decomposition of biomass takes place first and the radicals that are generated initiates the depolymerization of the plastic (Önal, Uzun, and Pütün 2014). Subsequently, the products from the decomposition reaction of the polyolefin prompts the interactions between the radicals and the bio char to produce 2-alkanes. The hydrogen from the plastic increases the degradation of cellulose in biomass and the oxygenated compounds in biomass promotes the cracking of plastics (Ryu et al. 2020).

The quality and yield of bio-oil products from pyrolysis process can be improved by the addition of catalyst support. In few previous studies, both zeolite and CaO catalysts have demonstrated excellent catalytic performance in the biomass pyrolysis (Imran et al. 2018; Fong et al. 2019). For instance, zeolite catalyst was able to decrease the content of oxygenated and other undesired compounds. The stability performance of bio-oil product was improved significantly as a higher amount aromatics content was found in the bio-oil during the reaction or regeneration cycles (Imran et al. 2018). Meanwhile, the CaO catalysts are widely used due to its inherent non-toxicity characteristic, low cost, and possess excellent ability to improve the quality of the biofuel (Wang et al. 2020). Furthermore, both Gan et al. (2018) and Fong et al. (2019) have found that the activation energy (E_A) of biomass pyrolysis was significantly lowered after the addition of CaO catalyst. Hence, such results highlighted that both zeolite and CaO catalysts exhibited positive catalytic effects on the pyrolysis process, especially those of using biomass as feedstock. However, to the best of the author's knowledge, no previous study has investigated the kinetic and thermodynamic behaviors of co-pyrolysis of microalgae *Chlorella vulgaris* and plastic high-density polyethylene (HDPE) waste mixtures over zeolite and CaO catalysts. Hence, the key objective of this research study was to investigate and compare the kinetic and thermodynamic behaviours of co-pyrolysis of microalgae *Chlorella vulgaris* and HDPE waste mixture over three types of catalysts, namely limestone (LS), zeolite HZSM-5, and bi-functional LS/HZSM-5 catalysts to investigate the potential of *Chlorella vulgaris* and HDPE mixture as a biofuel source. To scale up a process for commercial biofuel production, the kinetic parameters are crucial for the design of the pyrolysis reactor. The thermodynamic analysis tells how feasible the process is and what thermal conditions it will prefer. Therefore, it is essential to analyze the kinetic and thermodynamic behavior of the pyrolysis to design an optimized pyrolytic process, for an efficient conversion of any biomass and plastic waste mixtures to biofuel on an industrial level (Ahmad et al. 2017).

Microalgae *Chlorella*, being the third-generation biomass have many other advantages over first generation biomass and second generation biomass. Microalgae *Chlorella* is easy to cultivate and do not require arable land or freshwater to grow (Zullaikah et al. 2019). Microalgae bio-oil yield is 15–300 times more than that of traditional crops. Furthermore, microalgae biomass do not compete with food crops, are biodegradable and non-toxic (Hussian 2018). Meanwhile, HDPE is selected as a co-feedstock in the biomass pyrolysis process due to its advantage of having the least degree of branching compared to other types of polyethylene

(PE) and results to be easily broken down into smaller molecules with various chain length via the random chain scission when heat is applied (Kumar et al. 2011; Chin et al. 2014a).

Model-free methods such as Flynn–Wall–Ozawa, Kissinger, Kissinger-Akahira-Sunose, and Friedman generally allow the estimation of kinetic parameters without knowing the reaction mechanism. Kissinger-Kai method provides a better estimation of the kinetic parameters due to the introduction of multiple sub-reactions as compared to other model free methods (Li et al. 2014a). Model-fitting methods are typically used to fit the experimental thermogravimetric data into a simulated pyrolysis model. The model with the best statistically fitted experimental data is further considered for the calculation of kinetic parameters (Ding et al. 2019).

Typically, many model-fitting methods incorporate mathematical functions that relate closely to the reaction mechanism of a pyrolysis process. As the mathematical function becomes more complicated, the traditional model-fitting methods may fail to determination the kinetic parameters accurately. Therefore, various heuristic algorithms such as the Particle Swarm Optimization (PSO) heuristic algorithm, the Genetic Algorithm (GA), and Shuffled Complex Evolution (SCE) algorithms have been developed, and demonstrated to be feasible and highly effective. Among these conventional heuristic algorithms, PSO have gained much popularity as it incorporates the velocity and position of particles, which leads to faster and closer convergence to the optimum contrast to other algorithms (Ding et al. 2019). It is also highlighted that PSO demonstrates better optimization capacities with similar convergence solution to the global optimum and faster convergence to the solution primarily on the main components (hemicellulose, cellulose, and lignin) parallel reaction mechanism of biomass pyrolysis in comparison to GA (Ding et al. 2019). Due to such distinct advantages, it has been used by Ding et al. (2019) who has investigated the pyrolysis of pinewood based on the thermogravimetric analysis. From the optimized parameters, the predicted results were in good agreement with the experimental data and hence validated the high accuracy of the PSO method.

2.0 Materials and Methods

2.1 Samples preparation

The microalgae *Chlorella vulgaris* and HDPE were obtained from Universiti Teknologi PETRONAS (UTP) and Shen Foong Plastic Industries Sdn Bhd, respectively. The microalgae *Chlorella vulgaris* was composed of (8.3±0.3)% moisture, (59.2±1.9)% volatile matter, (15.8±2.1)% fixed carbon, and (16.7±1.3)% ash. On the other hand, the HDPE consisted of (99.5±0.4)% volatile matter and, (0.5±0.1)% ash. The proximate analysis was conducted using gravimetric analysis method adopted by Gracía et al. (2013). The fixed carbon was obtained based on the difference in calculation. For the preparation of the co-pyrolysis of binary mixtures, the microalgae *Chlorella vulgaris* and HDPE were homogenously mixed at a weight ratio of 0.8:0.2.

Powdered limestone (LS), HZSM-5 zeolite and bi-functional LS/HZSM-5 were prepared based on the methods adopted by Fong et al. (2019). The HZSM-5 zeolite catalyst was obtained from Sigma-Aldrich, Malaysia and the LS catalysts powder was purchased from Calrock Sdn. Bhd., Malaysia. All catalysts were added to the binary mixture of microalgae *Chlorella vulgaris* and HDPE at a weight ratio of 1:10.

2.2 Thermogravimetric Analysis Approach (TGA)

The pyrolysis experiments were performed in a thermogravimetric analyzer (EXSTAR TG/DTA 6300) at heating rates of 10, 20, 30, 50 and 100 °C/min. Prior to the pyrolysis process, the TGA equipment was flushed thoroughly with 100 mL/min pure nitrogen gas (N_2) for 20 minutes to ensure an inert atmosphere and to avoid any undesirable oxidation reaction of the sample. Subsequently, 5 mg of samples were placed in a crucible, before the temperature was increased from 50°C to 900°C under the respective heating rates and kept constant for 10 minutes.

2.3 Kinetic Analysis

2.3.1 Kissinger and Kissinger-Kai (K-K) method

The decomposition rate of solid materials can be expressed by the following equation:

$$\frac{d\alpha}{dt} = kf(\alpha) \quad (1)$$

where α is the conversion rate, t is the time (s) and k is the rate constant which is temperature dependant and can be expressed by the Arrhenius equation below;

$$k = A \exp\left(\frac{-E_A}{RT}\right) \quad (2)$$

where E_A is the activation energy (kJ/mol), A is the pre-exponential factor (s^{-1}) , R is the gas constant (8.314 J K^{-1} mol^{-1}), and T is the reaction temperature (K).

For pyrolysis, the reaction-order model, $f(a)$, can be written as

$$f(a) = (1 - a)^n \quad (3)$$

where n is the reaction order.

The final reaction rate can be expressed as:

$$\frac{d\alpha}{dt} = A\,(1-a)^n \exp\left(\frac{-E_A}{RT}\right) \tag{4}$$

The time derivative of the equation above at the peak location can be written as

$$\frac{E_A}{RT_p{}^2}\frac{dT}{dt} = An(1-a_p)^{n-1} \exp\left(\frac{-E_A}{RT_p}\right) \tag{5}$$

where T_p is the temperature corresponding with the peak of the derivative thermogravimetric (DTG) curve and a_p is the conversion rate at the peak.

For linear heating rate, $= \frac{dT}{dt}$, Kissinger (1957) considered that $n(1-a_p)^{n-1}$ was not dependent on β and its value was approximately 1. By taking the logarithm of the equation, the Kissinger equation can be written as:

$$\ln\left(\frac{\beta}{T_p{}^2}\right) = \ln\left(\frac{AR}{E_A}\right) - \frac{E_A}{R}\frac{1}{T_p} \tag{6}$$

The E_A and A can be found from the slope and intercept of the graph of $\ln\left(\frac{\beta}{T_p{}^2}\right)$ vs $\frac{1}{T_p}$, respectively.

The peak temperatures need to be determined in the next step. Biomass consists of different components and the decomposition process involves more than one reaction as concluded by many researchers after observing the multiple peaks and shoulders on the DTG curves of biomass pyrolysis (Hu, Jess, and Xu 2007). Mészáros et al. (2004) had described the pyrolysis reaction as independent components undergoing independent parallel reactions. Since lignocellulosic biomass contains cellulose, hemicellulose and lignin, therefore, the three pseudo-components parallel reaction model has been widely implemented by researches to describe the pyrolysis reaction mechanism (Hu, Jess, and Xu 2007). There are five main components of microalgae biomass; hemicellulose, cellulose, lignin, lipid and protein (Bui, Tran, and Chen 2015). Bui, Tran, and Chen (2015) had carried out the kinetic analysis of the pyrolysis of microalgae using the five pseudo-components model assumption and had concluded that the model was suitable for the simulation of microalgae pyrolysis. Therefore, the five pseudo-components model has been assumed in the present study and the reaction mechanism can be expressed as:

$$Hemicellulose \rightarrow\ v_1 char + (1 - v_1) volatiles$$

$$Cellulose \rightarrow\ v_2 char + (1 - v_2) volatiles$$

$$Lignin \rightarrow\ v_3 char + (1 - v_3) volatiles$$

$$Lipid \rightarrow\ v_4 char + (1 - v_4) volatiles$$

$$Protein \rightarrow\ v_5 char + (1 - v_5) volatiles \quad (7)$$

where *v* is mass fraction of char.

For pyrolysis reaction of plastic, only a single component was assumed to undergo the decomposition reaction. For the pyrolysis of the binary mixture, the number of components became 6 and the following reaction mechanism was included:

$$Plastic \rightarrow\ v_6 char + (1 - v_6) volatiles \quad (8)$$

Distinct peaks can be observed in the DTG graphs. Each peak represented different component and can be calculated using K-K method. The K-K method applied a second derivative of $\frac{m}{m_0}$ (DDTG) to determine the peak locations, estimate the kinetic parameters based on Kissinger method and provide a basis for the search range of the PSO optimization method:

$$|DDTG| = \left|\frac{d^2(\frac{m}{m_0})}{dT^2}\right| = \left|\sum_{i=1}^{6} Y_i \frac{d^2\alpha_i}{dT^2}\right| \geq 0 \quad (9)$$

where Y_i is the mass fraction of component *i*, α_i is the conversion rate of component *i*, m_o is the initial mass, and m is the mass at temperature *T*. The absolute value of the second derivative will drop exponentially to zero when the major component is near the maximum decomposition rate and the value of $|DDTG|$ usually drops promptly to a local minimum when there is no disturbance from other peaks nearby. As a result, the peak locations of the components can be obtained, and the values of E_A and *A* can be estimated by from the Kissinger equation.

An n-th order reaction-order model can be used to represent the reaction rate of each component:

$$\frac{dY_i}{dt} = -Y_{i,0}\left(\frac{Y_i}{Y_{i,0}}\right)^{n_i} A_i \exp\left(-\frac{E_{A,i}}{RT}\right)\ (i = 1,2,3,4,5,6) \quad (10)$$

The rate of production of char can be obtained by the following expression:

$$\frac{dY_{char}}{dt} = -\sum_{i=1}^{6} v_i \frac{dY_i}{dt} \quad (11)$$

The mass loss rate (mlr) is obtained by adding Eqs. (10) and (11) and then dividing by the heating rate, β :

$$MLR = \frac{d(\frac{m}{m_0})}{dT} = \frac{1}{\beta}\left(\sum_{i=1}^{6} \frac{dY_i}{dt} + \frac{dY_{char}}{dt}\right) \tag{12}$$

The total mass loss (m) can be obtained by integrating Eq. (12):

$$\frac{m}{m_0}\,(T) = 1 + \int_{T_0}^{T} MLR\; dT \tag{13}$$

where T_o is the initial temperature (K) and T is the final temperature (K).

2.3.2 Particle Swarm Optimization (PSO) Model

For each component, the five optimization parameters include $Y_{i,0}$, A_i, $E_{A,i}$, n_i, and v_i. As the initial mass fractions, $Y_{i,0}$ of the all components in a reaction should sum up to 1, hence the mass fraction of one component was calculated by difference. In total, there are 24 parameters for the 5-component parallel reaction mechanism of microalgae and 29 parameters for the 6-component parallel reaction mechanism of binary mixture. For pure plastic pyrolysis, only four parameters were optimized since the mass fraction of a single component was 1. PSO algorithm was used to predict the undefined kinetic parameters by using the velocity and position search model from a certain number of particles. By using the velocity and position of the particles, PSO helps to determine the updated position of the particles (Xu, Jiang, and Wang 2017). By comparing the differences between the predicted results and experimental data of mass loss and mass loss rate, the optimized position of each particle can be calculated by the following equations.

$$\varphi = \varphi_m + \varphi_{mlr} \tag{14}$$

$$\varphi_m = \sum_{j=1}^{N}\left[w_{CML,j} \frac{\sum_{k=1}^{\lambda}\left(CML_{pred,k} - CML_{exp,k}\right)^2}{\sum_{k=1}^{\lambda}\left(CML_{exp,k} - \frac{1}{\lambda}\sum_{p=1}^{\lambda} CML_{exp,p}\right)^2}\right] \tag{15}$$

$$\varphi_{mlr} = \sum_{j=1}^{N}\left[w_{MLR,j} \frac{\sum_{k=1}^{\lambda}\left(MLR_{pred,k} - MLR_{exp,k}\right)^2}{\sum_{k=1}^{\lambda}\left(MLR_{exp,k} - \frac{1}{\lambda}\sum_{p=1}^{\lambda} MLR_{exp,p}\right)^2}\right] \tag{16}$$

where, φ_m and φ_{mlr} are the objective functions for mass loss and mass loss rate, respectively. MLR and CML represent the mass loss rate and cumulative mass loss, respectively. λ is the number of experimental data points for each experiment, N is the number of experiments, and $w_{CML,j}$ and $w_{MLR,j}$ are the weighted values which are set to 1 in this model. The subscripts ‘pred’ and ‘exp’ represent the predicted and experimental values, respectively.

As the historical position vector and global best position best position were maintained by each particle, the equations below can be used to improve a particle's historical position vector and global best position best position (Buyukada 2016):

$$v_{id}{}^{k+1} = \omega v_{id}{}^{k} + c_1 r_1 (p_{id} - x_{id}{}^{k}) + c_2 r_2 \left(p_{gd} - x_{id}{}^{k}\right) \tag{17}$$

$$x_{id}{}^{k+1} = x_{id}{}^{k} + v_{id}{}^{k+1} \tag{18}$$

where *i* is the particle number, *k* is the iteration number, *d* is the search direction (from 1 to D), *w* is the inertia weight, p_{id} is the best individual particle position, p_{gd} is the global best position for all the particle. The c_1 and c_2 are two positive acceleration constants, which represent the personal and global nature of the swarm r_1 and r_2 are 2 random values in the range of [0,1].

2.4 Thermodynamic Analysis

Thermodynamic parameters include change in entropy (ΔS), enthalpy (ΔH), and Gibb's free energy (ΔG) were determined from the E_A values.

The parameters can be obtained by using the following equations:

$$\Delta H = E_A - RT \tag{19}$$

$$\Delta G = E_A - RT_m ln\left(\frac{K_B T_m}{hA}\right) \tag{20}$$

$$\Delta S = \frac{\Delta H - \Delta G}{T_m} \tag{21}$$

where *h* is Plank constant (6.626×10^{-34} J), K_B is Boltzman constant (1.381×10^{-23} J K^{-1}), and T_m (K) represent the average peak temperature in the differential thermogravimetric (DTG) profiles.

2.5 Sensitivity Analysis

The kinetic optimization parameters in this study are considered to have an impact on the final predicted results. Hence, a sensitivity analysis was required to determine which input parameter had the most significant effect on the output. There are two techniques that can be used to perform sensitivity analysis i.e. local sensitivity analysis and global sensitivity analysis. Local sensitivity analysis evaluates the local output response by changing a single input parameter at a time while the other parameters are kept at central values. Even though the local sensitivity analysis is an easy technique to use, it can only examine one point at a time. In contrast, global sensitivity analysis eliminates this limitation by examining the model's global response to the variance of all input parameters.

To perform global sensitivity analysis, most commonly used method is sampling-based method. In specific, the Latin Hypercube Sampling (LHS) method was developed by Mckay, Beckman, and Conover (2000) and it has demonstrated to improve performance in terms of versatility, implantation, and adaptability of sensitivity analysis. Random samples can be generated from multiple dimensions using the LHS method which follows the Latin square design, putting one single sample in each row and each column in a multidimensional (hypercube) cube. The key principle is the stratification of the input probability distribution where the cumulative curve is divided into equal intervals (Olsson, Sandberg, and Dahlblom 2003). Only one single sample is then randomly taken from each interval or stratification. For an n-dimensional sampling, the *n* number of variables are independent of each other. One-dimensional LHS samples are generated for each variable and the samples are combined to form multi-dimensional sets (Xin Li 2014). The LHS allows extraction of a significant amount of sensitivity and uncertainty information from a very small sample size. Moreover, the rank-transformation is usually applied to LHS samples and the data can be used to normalize the underlying correlation between the input parameters and expected value of the output, φ. This raw sampled data of the inputs and outputs is then replaced by their rank of transformation. Lastly, Spearman rank correlation coefficient is used to represent the correlation between the kinetic parameters (inputs) and predicted results (output). The correlation equation can be expressed as follows:

$$\rho = 1 - \frac{6}{s(s^2-1)} \sum_{i=1}^{s} (R_i - Q_i)^2 \qquad (22)$$

where *s* is the sample number, *R* is the rank of input value, and *Q* is the rank of output value.

3.0 Results and Discussion

3.1.1 Thermal degradation behaviour of pure microalgae *Chlorella vulgaris* and pure HDPE

Fig(s) 1a and 1b illustrate the thermogravimetry (TG) and the derivative thermogravimetry (DTG) profiles for microalgae *Chlorella vulgaris* at heating rates of 10-100 °C/min. The TG and DTG curves were divided into the three volatilization stages, namely Stage I, Stage II, and Stage III.

From Fig(s) 1a and 1b, Stage I of the pyrolysis of *Chlorella vulgaris* occurred from 34°C to 150°C with a small percentage weight loss of 8.26%–11.67%. Such mass loss can be attributed to the moisture removal from the biomass. Therefore, Stage I is known as the moisture drying or the dehydration stage (Gan et al. 2018) . This drying process corresponded to the first peak in the DTG curve. The Stage II, also known as the main de-volatilization, occurred between temperatures from 150°C to 580°C. Most of the weight loss (47.53-51.88%) occurred in this stage associated with the decomposition of lipids, proteins, and carbohydrates. In Stage II, the highest peak corresponded to the decomposition of protein and carbohydrates, while the lower peak corresponded to the degradation of lipids (Fong et al. 2019). For Stage III, it took place between 580°C-900°C. The percentage weight loss in this stage was ranged between 27.04%-7.78% which was due to the degradation of strong aromatic rings in lignin such as benzene and phenol and other carbonaceous constituents within the solid residues (Bach and Chen 2017). The small peak in the DTG curves at around 750°C-850°C represented the decomposition of carbonaceous materials and lignin. A residual mass of 13.76%-32.58% was left after the decomposition.

An upward shift pattern in the TG and DTG curves was observed with increasing heating rates. A lateral shift of the TG curve to the right at higher heating rate indicated a longer reaction time was required to break down the volatile matters. The heating rates also seemed to affect the maximum decomposition rate. The DTG curve gave higher peaks at higher heating rates. Table 1 shows the maximum degradation temperatures (T_{max}) at different heating rates, where T_{max} was observed to be increased at higher heating rates. Similar findings were also found in Fong et al. (2019) who investigated the pyrolysis of microalgae *Chlorella vulgaris.*

The TG and DTG curves of HDPE at different heating rates are shown in Fig(s) 1c and 1d, respectively. It can be observed from the TG curves that the thermal degradation commenced at about 230°C-260°C and was almost completed around 480°C-590°C. In the DTG profiles, only one significant peak was observed in the heating temperature of 230°C-590°C. Therefore, it can be concluded that the decomposition of HDPE took place in a single stage. Similar observation in the DTG curves of HDPE was also reported by Chin et al. (2014b) who performed pyrolysis of rubber seed shell and HDPE. In this study, the percentage of weight loss of HDPE was reported in the range of 94.9-97.98%. The maximum degradation rate was increased from 18.03 %/min to 128.2 %/min as the heating rates were increased from 10°C/min to 100°C/min. The decomposition temperatures of HDPE were also observed to be higher than the decomposition temperatures of microalgae *Chlorella vulgaris*.

3.1.2 Thermal degradation behaviour of non-catalytic and catalytic pyrolysis of microalgae Chlorella vulgaris and HDPE binary mixture

The TG and DTG curves of microalgae *Chlorella vulgaris* and HDPE mixtures are illustrated in Fig(s) 2a and 2b, respectively. It can be observed that the maximum degradation temperatures of the binary mixtures at different heating rates improved with increasing heating rate. Also, it can be observed that the maximum degradation rate of the binary mixtures was less to the maximum rate of pristine HDPE. On the contrary, the maximum degradation rate of the binary mixture was higher than of *Chlorella vulgaris* alone. As seen in Table 1, the maximum loss rate was 86.39wt%/min at 100^{o}C/min. Under the same heating rate, the maximum rate of loss was 128.2wt%/min for HDPE and 21.05%/min for microalgae *Chlorella vulgaris*. At the main de-volatilization stage, the total mass loss of the binary mixture was 78.28%-90.96%, whereas the total mass loss of *Chlorella vulgaris* and HDPE were 47.53%-51.88% and 94.9%-97.98%, respectively. Furthermore, the pyrolysis of *Chlorella vulgaris*/HDPE mixture produced less residues (6.43-12.02%) than the pyrolysis of *Chlorella vulgaris* (13.79-32.58%), mainly due to the addition of HDPE in the mixture. Rotliwala and Parikh (2011) made the similar observations in the study of co-pyrolysis of rice-bran with HDPE.

The degradation of hemicellulose occurred in the first stage, the decomposition of cellulose carried out in the second stage, and the decomposition of lignin and HDPE took place in the third stage. The TG and DTG graphs show similar characteristics in this study with two different slope shapes of the TG curves in the main decomposition stage and DTG graphs showing one group of peaks occurring between 200-400°C and another group of peaks occurring between 400-600°C. The peaks in the region between 200-400°C are not distinct and cannot be observed easily. According to Yang et al. (2007), the degradation temperature range falls between 200-300°C for hemicellulose and 300-400°C for cellulose. According to Bui, Tran, and Chen (2015), lipid and protein decomposition also occur between 200-400°C. Therefore, it can be said that hemicellulose, cellulose, lipid, and proteins are responsible for the peaks in this region in the DTG graphs. The peaks occurring between 400-600°C are easily distinguishable, and they can be said to represent the degradation of lignin and HDPE.

Fig. 2 illustrates the TG and DTG curves of microalgae *Chlorella vulgaris* and HDPE mixtures over the LS catalyst (Fig(s) 2c and 2d), HZSM-5 catalyst (Fig(s) 2e and 2f), and LS/HZSM-5 catalyst (Fig(s) 2g and 2h). From the DTG curves, it can be seen that the maximum degradation temperatures at different heating rates improved with increasing heating rates. From the main de-volatilization stage, it can also be observed that the maximum degradation rate and total mass loss were significantly lower than that of the non-catalytic pyrolysis. For Table 1, the maximum mass loss rate of non-catalytic pyrolysis of *Chlorella vulgaris/HDPE* mixture was 86.39 wt%/min. Under the same heating rate of 100°C/min, the maximum mass loss rates of the same binary mixture over LS, HZSM-5 and LS/HZSM-5 catalysts were reduced to 26.66 wt%/min, 32.25 wt%/min and 33.8 wt%/min, respectively. In the main de-volatilization stage, the total mass loss for non-catalytic pyrolysis was 71.4-82.9% whereas the total mass losses for catalytic pyrolysis using LS, HZSM-5, and LS/HZSM-5 catalysts were 58.63-63.93%, 67.97-70.78%, and 54.19-70.21%, respectively. As a result, the catalytic reaction produced more residues (17.67-26.09%) than the non-catalytic pyrolysis (6.43-12.02%).

A single peak was observed in the temperature range of 576-899°C in the DTG curves of the catalytic pyrolysis. On the other hand, no peaks can be seen in the same temperature range for the non-catalytic pyrolysis. Besides the decomposition of carbonaceous materials, the DTG curve peaks at Stage III for catalytic pyrolysis using LS and LS/HZSM-5 also occurred due to the decomposition of $CaCO_3$. According to Abunowara and Elgarni (2013), the carbonation of CaO into $CaCO_3$ occurred in the temperature range of 550–750°C. Therefore, the small DTG curve peaks in Stage III represented the carbonation of CaO to $CaCO_3$. $CaCO_3$ was subsequently converted back to CaO at the end of the pyrolysis reaction when the temperature exceeded the carbonation temperature and reached 900°C (Gan et al. 2018).

In this study, the maximum degradation rate of the catalytic pyrolysis of *Chlorella vulgaris*/HDPE mixture was found to be lower than the maximum degradation rate of non-catalytic pyrolysis. As seen in Table 1, for the heating rate of 100°C/min, the maximum degradation of rate *Chlorella vulgaris*/HDPE mixture was found to be 86.39 wt%/min, whereas the maximum degradation of the binary mixture in the presence of LS, HZSM-5, and bi-functional LS/HZSM-5 catalysts were 26.66 wt%/min, 32.25 wt%/min, and 33.8 wt%/min, respectively. Previous studies also observed the same phenomena during the catalytic pyrolysis of biomass (Fong et al. 2019). A reduction in the maximum degradation rate was reported after the addition of catalysts, and the rate of reaction was found to be improved substantially.

3.2 Effect of Heating Rate on the Thermal Degradation

The TG and DTG curves of all samples showed an upward shift pattern with an increase in the heating rates. The higher the heating rate, the faster the maximum decomposition rate achieved for each sample, as shown in Table 1. The maximum decomposition rate of *Chlorella vulgaris* increased from 2.20-21.05 %/min when the heating rate was increased from 10 to 100 °C/min, and the same trend was observed in other samples. The same observation was reported in the work by Fong et al. (2019). The TG and DTG curves also depicted a lateral shift to the right as the heating rate increased. In other word, a longer reaction time was required to achieve the minimum energy for the decomposition reaction to begin. The incremental temperatures from the initial, final, and maximum peak of the main de-volatilization stage with increasing heating rates were observed in Table 1.

It is evidenced that a shorter sample's residence time in the TGA helps to improve the rate of decomposition as the heating rate increased. Since biomass is a poor heat conductor, the heat transfer through the sample can be regarded as considerably low and a higher heating rates could promote a steeper cross-sectional temperature gradient of the sample. Moreover, a low heating rate is more likely to promote secondary reactions such as de-polymerization, cracking, and re-condensation, resulting in char formation due to prolonged residence time (Fong et al. 2019). Therefore, it can be concluded that a high heating rate can intensify the thermal energy within the sample and promotes the heat transfer performance in the pyrolysis of biomass and plastic mixture.

3.3 Effect of Catalyst on the Thermal Degradation

In this study, the main rationale of adding catalyst into the biomass pyrolysis reaction was to improve quality of the pyrolysis products and to lower the E_A of the reaction process. Furthermore, the in-situ catalytic pyrolysis of microalgae has not been studied as compared to the catalytic pyrolysis of conventional biomass (Hu et al. 2011). In the literature, the microalgae *Chlorella vulgaris* has been reported to produce a complex mixture of bio-oil product containing ethers, phenolics, acids and aromatic alkanes, which was derived from the decomposition of carbohydrate, protein, and lipids (Bong et al, 2020). In previous studies, the catalytic effect of LS powder was investigated in the pyrolysis of rice hull and it was observed that the E_A of the catalytic pyrolysis was significantly lower than the non-catalytic pyrolysis (Gan et al. 2018). The same result was achieved by Fong et al. (2019) who performed catalytic pyrolysis of microalgae *Chlorella vulgaris* over LS, HZSM-5 and bi-functional LS/HZSM-5 catalyst. The E_A of the catalytic pyrolysis was found to be significantly lower than the E_A of the non-catalytic pyrolysis of *Chlorella vulgaris*. Furthermore, it was noticed that the LS/HZSM-5 had a better catalytic effect as compared to LS and HZSM-5 catalysts.

In the present study, one can be noticed that the maximum decomposition peaks of microalgae *Chlorella vulgaris* and HDPE mixture over the catalysts were lower than the maximum decomposition peaks of the non-catalytic pyrolysis of the binary mixture. The maximum degradation rate of the non-catalytic binary mixture was 12.61%/min whereas the maximum degradation rate of the catalytic pyrolysis over LS, HZSM-5, and the bi-functional LS/HZSM-5 were 4.32%/min, 3.94%/min and 4.50 %/min, respectively, for a heating rate of 10 °C/min. The same observation was reported by Fong et al. (2019), where the maximum degradation rate decreased after the addition of catalysts.

3.4 Kinetic Analysis

To obtain the kinetic parameters, the peak temperatures of each components should be located at its respective maximum decomposition rates of the different components. The DTG graphs of *Chlorella vulgaris* only three distinguishable peaks can be identified; therefore, assumptions were made based on the thermogravimetric analysis of *C. sorokiniana* by Bui, Tran, and Chen (2015). It was reported that the cellulose was responsible for the highest peak in the DTG graph. In the same temperature range as cellulose, the peaks for hemicellulose (230°C-330°C) and protein (230°C-390°C) were found to be overlapped with cellulose (250°C-350°C) and could not be distinguished in the DTG graph. The second highest peak as noticed at around 380°C which was responsible for the decomposition of lipid. A shoulder was observed around 430°C, which was responsible for the decomposition of lignin. Fong et al. (2019) also reported that the highest peak in the main decomposition stage of *Chlorella vulgaris* occurred due to the decomposition of carbohydrates and proteins, whereas, the second-highest peak indicated the decomposition of lipids. For this study, only the main decomposition stage was analysed. The first peak, second peak, and third peak in the DTG curve of pure *Chlorella vulgaris* was assumed from the decomposition of cellulose, lipid, and lignin, respectively. In the DTG graph of pyrolysis of binary mixtures, the peak responsible for the decomposition of HDPE was assumed to be the last peak in the main decomposition stage as the thermal degradation of HDPE occurred in the temperature range of 470-510 °C in the pyrolysis of pure HDPE. In the kinetic study of co-pyrolysis of rubber seed shell (RSS) with HDPE by Chin et al. (2014b), the peak responsible to the decomposition of HDPE only appeared followed by the peaks which were responsible for biomass decomposition. Thus, one can assume that the HDPE decomposed the last in the pyrolysis reaction and gave rise to the last peak in the DTG curves in the present study.

After the peak temperatures for the cellulose, lipid, lignin, and HDPE were identified, the graphs of $\ln(\beta/T_p^2)$ vs $1000/T_p$ was plotted using the Kissinger equation. The E_A and A values were calculated using the gradient and the y-intercept values of the graphs. The calculated kinetic parameters are tabulated in Table 2. The E_A and A values of hemicellulose and protein were obtained from literature from the pyrolysis of *Chlorella sorokiniana* conducted by Bui, Tran, and Chen (2015).

The search range for particle swarm optimization was established based on the calculated values for the kinetic parameters using K-K method. As the peaks representing cellulose, lignin, and lipid were identified in this study, the initial values for the E_A and the A of hemicellulose and protein were taken from the literature. The initial mass fractions $Y_{i,0}$ of all the components were assumed using the chemical composition of *Chlorella vulgaris* as aforementioned in Section 3.1, where the percentage of protein, lipid, and carbohydrates were 53.1 wt%, 26.7 wt% and 12.3 wt%, respectively. The remaining 7.9 wt% was assumed to be lignin. The initial values for the char yields of cellulose, hemicellulose, and lignin were taken from Ding et al. (2019), whereas the char yields of protein and lipid were assumed to be the same as the char yield of lignin. On the other hand, the char yield of HDPE was obtained from the experimental data, which was the average value of percentage mass remaining (4.0 %) for the TGA experiments at different heating rates. The lower and upper bounds of the PSO search range for E_{Ai}, A_i, Y_{io} and v_i were set from 50 to 150% of the initial values. The initial value for the reaction order (n) was assumed to be 1 and the search range for n was set from 0 to 5. The optimized mass fraction of hemicellulose was calculated by adding all the optimized mass fractions of all the other components and subtracting from 1. Based on the literature, the PSO optimization produced the best fitting when the swarm size was set to 2,500 with 10,000 iterations (Ding et al. 2019). However, in the present study, both the swarm size and the number of iterations were kept at 50 due to time constraint.

For the catalytic pyrolysis of *Chlorella vulgaris* and HDPE mixture over bi-functional LS/HZSM-5 catalyst, the optimized parameters generated by the PSO are listed in Table 3 as an example. The graphs for the experimental mass loss rate (mlr) versus the predicted mlr and the experimental cumulative mass loss (cml) vs the predicted cml were plotted for each sample under the heating rate of 10°C/min with and without catalysts in Fig 3. As seen from Fig. 3, the predicted cml and the experimental cml were in good agreement with each other with the R^2 value ranging from 0.9138 to 0.9920. However, the predicted mlr showed some discrepancies when compared with the experimental mlr, especially for *Chlorella vulgaris*, HDPE and *Chlorella vulgaris*/HDPE mixture. The R^2 values for these three samples were in the range of

0.1719 to 0.5374. The predicted mlr data and the experimental mlr data of the biomass and plastic mixture over the catalysts gave R^2 values in the range of 0.7203 to 0.7773, which still considered as acceptable.

Such significant difference between the predicted and experimental result can be explained by the swarm size and the number of iterations. To verify this finding, the graph of predicted results versus experimental results prior optimization was plotted for microalgae *Chlorella vulgaris* and *Chlorella vulgaris*/HDPE mixture and illustrated in Fig(s) 4a and 4b, respectively. It can be seen there was an apparent deviation between the experimental and predicted cml graphs and the R^2 values were reduced from 0.9138 to 0.8476 and 0.9219 to 0.8589, respectively. The R^2 values of the mlr of *Chlorella vulgaris* and *Chlorella vulgaris/*HDPE mixture were reduced from 0.4369 to 0.3594 and 0.1719 to 0.0938, respectively. This finding agrees with the observation made by Ding et al. (2019) in the study of kinetic parameters estimation for the pyrolysis pinewood using PSO when they compared the results before and after optimization. Hence, one can conclude that the kinetic parameters of the pyrolysis reaction of any biomass or plastic waste can be predicted accurately by increasing the swarm size and the iteration number.

The kinetic analysis was studied by using the K-K method coupled with PSO for the catalytic and non-catalytic pyrolysis of *Chlorella vulgaris*, HDPE and *Chlorella vulgaris*/HDPE mixture. The optimized E_A, A and n values for all samples are tabulated in Table 4. The E_A values of hemicellulose, cellulose, lignin, lipid, and protein were found to be 117.27 kJ/mol, 183.86 kJ/mol, 269.65 kJ/mol, 233.55 kJ/mol and 118.66 kJ/mol, respectively for the pyrolysis of *Chlorella vulgaris*. These values are in good agreement with the values found in the literature. In general, the E_A of hemicellulose varies between 105-117 kJ/mol and the E_A of cellulose varies between 195–213 kJ/mol (Manyà, Velo, and Puigjaner 2003; Grønli, Várhegyi, and Di Blasi 2002; S. Hu, Jess, and Xu 2007; Bui, Tran, and Chen 2015). The E_A of lignin ranges from 59–361 kJ/mol in many previous studies. (Ferdous et al., 2002; Ház et al., 2019; Avni and Coughlin 1985). In the study of pyrolysis of *Chlorella vulgaris*, Phusunti (2012) found that the E_A of lipid extracted from *Chlorella vulgaris* was found about 200 kJ, which is comparable to the E_A calculated for *Chlorella vulgaris* lipid (233.55 kJ) in the present study. To compare the E_A and A values of the catalytic and non-catalytic pyrolysis, an average of the E_A and A values was obtained for all samples. It was found that the average E_A and A values of *Chlorella vulgaris* were 184.6 kJ/mol and 5.44×10^{17} s^{-1}, respectively. The E_A and A of pyrolysis of *Chlorella vulgaris* found in Fong et al. (2019) were 156.16 kJ/mol and 4.83×10^{18} s^{-1}, respectively. The estimated E_A and A for HDPE was found to be 253.79 kJ/mol and 5.01×10^{14} s^{-1} in this study. In literature, the E_A and A of HDPE were found to be ranging from 242.13-278.14 kJ/mol and 8.3×10^{18}-1.05×10^{22} s^{-1} (Chin et al. 2014b).

The average E_A and A values of microalgae *Chlorella vulgaris* and HDPE mixture 170.36 kJ/mol and 6.38×10^{15} s^{-1}, respectively. Therefore, the E_A of the mixture was substantially to be lower than the E_A of the pyrolysis of the individual components. Also, the A values of the binary mixture was found to be lower than the A value of the pure *Chlorella vulgaris* but higher than the A value of the pure HDPE. This shown that both *Chlorella vulgaris* and HDPE interacted with one another during the decomposition reaction, thereby changing the reaction kinetics. The same phenomenon was observed by Chin et al. (2014b) in the pyrolysis of rubber seed shell and HDPE mixture where the E_A and A values of the binary mixture were lower than the E_A and A values of pure HDPE but marginally higher than of to pure biomass.

The presence of catalyst in the pyrolysis reaction significantly lowered the E_A of the *Chlorella vulgaris* and HDPE mixture. It can be seen that the calculated values using K-K method for cellulose, lignin, lipid, and HDPE were lower for the catalytic pyrolysis of the binary mixture, thereby lowering the average value of the samples. As the E_A and A values of hemicellulose and protein could not be identified using the DTG graphs, the initial values in the PSO optimization were kept same for these two components for all the samples. As seen in literature, the PSO optimizer usually changes the E_A and A values of all components in order to fit the experimental data accurately. In the pyrolysis of pinewood, the initial E_A value of hemicellulose, cellulose and lignin were 155.99 kJ/mol, 156.94 kJ/mol, and 174.40 kJ/mol, respectively (Ding et al. 2019). The optimized values for hemicellulose, cellulose, and lignin after 10,000 iterations were 88.13, 157.67, and 136.60 kJ/mol, respectively (Ding et al. 2019). In another study, Ni et al. (2020) analyzed the pyrolysis kinetics of expanded polystyrene (EPS) by coupling the Flynn–Wall–Ozawa kinetic model with the PSO optimization method. The optimized E_A, A and n values of EPS were 170.10 kJ/mol, 3.34×10^{10} s^{-1} and 0.58, respectively.

Since the number of iterations in this study was only 50, therefore, the changes in the E_A and A values were insignificant for most components. Hence, the E_A and A values of hemicellulose and protein are incomparable for the catalytic and non-catalytic co-pyrolysis. The average E_A values of catalytic pyrolysis over LS, HZSM-5, and LS/HZSM-5 catalysts were 100.09 kJ/mol, 87.42 kJ/mol, and 83.59 kJ/mol, respectively. The average *A* values of catalytic pyrolysis in the presence of LS, HZSM-5 and LS/HZSM-5 catalysts were 5.85×10^8, 4.08×10^8 and 4.03×10^8 s^{-1}, respectively. Fong et al. (2019) also observed that LS, HZSM-5 and LS/HZSM-5 catalysts were capable to reduce the E_A of *Chlorella vulgaris* during the pyrolysis reaction. This catalytic effect reduces the minimum energy requirement provides better energy efficiency during bio-oil production via catalytic pyrolysis (Xu et al., 2017). The *A* value indicates the degree of the collision between the molecule during the pyrolysis reaction. Higher *A* value also refer to a greater amount of heat is required to achieve a higher molecular collision (Mong et al., 2019). Therefore, the determination of *A* values is essential to achieve an optimized biomass pyrolysis process. Hence, the addition of a catalyst is beneficial as it can lower both the minimum energy required to start a reaction and the energy required for molecules to collide with each other and continue the reaction. The *n* values for all the components were between 0.85-4.75. The reaction order values were in between 1 to 4 as reported in previous studies (Ding et al., 2019; Bui, Tran, and Chen 2015). According to Bui, Tran, and Chen (2015), the fit of a kinetic model is more accurate when *n* is not equal to 1.

3.5 Thermodynamic Analysis

The thermodynamic parameters for the catalytic and non-catalytic pyrolysis of *Chlorella vulgaris*, HDPE, the *Chlorella vulgaris*/HDPE mixture such as the change of enthalpy (ΔH), the change of Gibb's free energy (ΔG) and the change of entropy (ΔS) were calculated and presented in Table 5. The ΔH indicates the total energy utilized by the sample during the decomposition reaction and the formation of volatile and char products. According to Ahmad et al. (2017), a smaller difference between the ΔH and E_A values of a chemical reaction can lower the potential energy barrier and promote the formation of an activated complex. In this study, the small differences between the ΔH and E_A (4.3-6.3 kJ/mol) were observed for all the pyrolysis samples. This suggests that the pyrolysis reactions were feasible and products such as bio-oil or syngas production were more favourable formed in an energy-efficient way (Loy et al. 2019). As seen from Table 5, the ΔH was positive for all the samples which further confirms that the pyrolysis reactions were endothermic. The chemical bonds were broken and formed by absorbing heat from the system. Also, the ΔH values were around 180, 250, and 160 kJ/mol for the pyrolysis of *Chlorella vulgaris*, HDPE, and *Chlorella vulgaris*/HDPE mixture, respectively. For the catalytic pyrolysis using LS, HZSM-5, and LS/HZSM-5 catalysts, the ΔH values were around 95, 81, and 78 kJ/mol, respectively.

During a thermal reaction, the ΔG value indicates the stored energy in the reactants and helps to determine the total increase in energy of the thermodynamic system during the activated complex formation. A higher ΔG value indicates that a higher amount of energy is absorbed by the system during the reaction, whereas a lower ΔG value means the products can be formed with from a lower energy supply. This parameter can influence ΔH *and* ΔS of activated complex formation which will indirectly influence the bio-oil or syngas production. The ΔG values were calculated as 140, 230, and 130 kJ/mol for the pyrolysis *Chlorella vulgaris*, HDPE, and *Chlorella vulgaris*/HDPE mixture, respectively. For the catalytic pyrolysis using LS, HZSM-5, and LS/HZSM-5 catalysts the ΔG values were around 160, 157, and 147 kJ/mol, respectively. These values show that all the samples have the potential to undergo pyrolysis for biofuel production. In previous studies, the ΔG values of the pyrolysis of *Chlorella vulgaris* was found to be in the range of 129–206 kJ/mol.

The ΔS value is used to determine the degree of disorder in a system. In the present study, the ΔS values were positive for the pyrolysis of microalgae *Chlorella vulgaris*, HDPE and the binary mixture, whereas the ΔS values were all negative for the catalytic pyrolysis of the binary mixture. A negative ΔS value suggests that the reaction has reached thermal equilibrium, and the products are thermally stable. Meanwhile, a high ΔS means that the system has not reached equilibrium yet and can respond to a faster reaction rate if the reaction time is reduced. As seen from Table 5, the ΔH, ΔG and ΔS did not differ significantly when the heating rates were increased from 10 °C/min to 100 °C/min.

3.6 Sensitivity Analysis

The 29 parameters PSO model were used to conduct a sensitivity analysis. In this this sensitivity study, only the experimental data for the pyrolysis of microalgae *Chlorella vulgaris* and HDPE mixture with LS/HZSM- 5 catalyst was used. About 20,000 sets of the 29 kinetic parameters were sampled using LHS before used for rank transformation. The first 20 sets of the sampled and ranked parameters is shown in Table 6. The Spearman rank correlation was used to calculate the value of ρ for each kinetic perimeter based on the predicted results of Φ and as shown in Fig. 5. It can be observed that the parameters with the highest effect on the predicted results were the activation energy, E_c of cellulose, pre-exponential factor, ln A_c of cellulose and the activation energy, E_p of protein followed closely by the reaction order of cellulose, n_c. The results of the sensitivity analysis indicate that these parameters should be taken into careful consideration during the application of kinetics in the pyrolysis modelling of *Chlorella vulgaris* and HDPE mixture over the LS/HZSM- 5 catalyst.

4.0 Conclusion (100 words)

The co-pyrolysis of *Chlorella vulgaris/*HDPE mixture was investigated with the presence of LS, HZSM-5, and bi-functional LS/HZSM-5 catalysts. The bi-functional LS/HZSM-5 catalyst with the lowest E_A and ΔH values was found to be the most effective catalysts in the co-pyrolysis. This indicated a better thermochemical conversion pathway as compared to the latter two catalysts. A novel method that combined both Kissinger-Kai model-free method and PSO base model-fitting method was introduced to determine the pyrolysis kinetic parameters. Additionally, Latin Hypercube Sampling and rank transformation were compared in the global sensitivity analysis to evaluate the kinetic parameters based on three-parallel reaction mechanism.

Acknowledgments

The authors would like to express their sincere gratitude to the Curtin University Malaysia and the Centre of Biofuel and Biochemical (CBBR) of Universiti Teknologi PETRONAS (UTP) for the technical support. Furthermore, support from Ministry of High Education Malaysia through HICOE award to CBBR is duly acknowledged. Lastly, KWC acknowledge the EPSRC (EP/P034667/1) for partial funding.

References

1. Abunowara, M., Elgarni, M., 2013. Carbon dioxide capture from flue gases by solid sorbents. Energy Procedia 37:16–24.
2. Ahmad, M. S., Mehmood, M. A., Taqvi, S.T.H., Elkamel, A., Liu, C.G., Xu, J., Rahimuddin, S.A., Gull, M., 2017. Pyrolysis, kinetics analysis, thermodynamics parameters and reaction mechanism of *Typha latifolia* to evaluate its bioenergy potential. Bioresourc. Technol. 245: 491–501.
3. Avni, Eitan, Coughlin, R.W., 1985. Kinetic analysis of lignin pyrolysis using non-isothermal tga data. Thermochim. Acta 90: 157–167.
4. Bach, Q.V., Chen W.H., 2017. A comprehensive study on pyrolysis kinetics of microalgal biomass. Energy Convers. Manag. 131: 109–116.
5. Bong, J.T., Loy, A.C.M., Chin, B.L.F., Lam, M.K, Tang, D.K.H., Lim, H.Y., Chai, Y.H., Yusup, S., 2020. Artificial neural network approach for co-pyrolysis of *Chlorella vulgaris* and peanut shell binary mixtures using microalgae ash catalyst. Energy 207: 118289.
6. Bui, H.H., Tran, K.Q., Chen, W.H., 2015. Pyrolysis of microalgae residues - a kinetic study. Bioresour. Technol. 199: 362–366.
7. Buyukada, M., 2016. Co-combustion of peanut hull and coal blends: artificial neural networks modeling, particle swarm optimization and monte carlo simulation. Bioresour.

Technol. 216: 280–286.

8. Chin, B.L.F., Yusup, S., Al Shoaibi, A., Kannan, P., Srinivasakannan, C., Sulaiman, S.A., 2014a. Comparative studies on catalytic and non-catalytic co-gasification of rubber seed shell and high density polyethylene mixtures. J. Clean. Prod. 70: 303-314.

9. Chin, B.L.F., Yusup, S., Al Shoaibi, A., Kannan, P., Srinivasakannan, C., Sulaiman, S.A., 2014b. Kinetic studies of co-pyrolysis of rubber seed shell with high density polyethylene. Energy Convers. Manag. 87: 746–753.

10. Ding, Y., Zhang Y., Zhang, J., Zhou, R., Ren, Z., Guo, H., 2019. Kinetic parameters estimation of pinus sylvestris pyrolysis by Kissinger-Kai method coupled with particle swarm optimization and global sensitivity analysis. Bioresourc.Technol. 293: 122079.

11. Ferdous, D, Dalai, A.K., Bej, S.K.,Thring, R.W.,. 2002. Pyrolysis of lignins: experimental and kinetics studies. Energy Fuels 16: 1405–1412.

12. Fong, M.J.B., Loy, A.C.M., Chin, B.L.F., Lam, M.K., Yusup, S., Jawad, Z.A., 2019. Catalytic pyrolysis of *Chlorella vulgaris*: kinetic and thermodynamic analysis. Bioresourc. Technol. 289: 121689.

13. Gan, D.K.W., Loy, A.C.M., Chin, B.L.F., Yusup, S., Unrean, P., Rianawati, E., Acda, M.N., 2018. Kinetics and thermodynamic analysis in one-pot pyrolysis of rice hull using renewable calcium oxide based catalysts. Bioresourc. Technol. 265: 180–190.

14. García R., Pizarro C., Lavín, A.G., Bueno, J.L., 2013. Biomass proximate analysis using thermogravimetry. Bioresourc. Technol. 139: 1-4.

15. Grønli, M.G., Gábor V., Di Blasi, C., 2002. Thermogravimetric analysis and devolatilization kinetics of wood. Ind. Eng. Chem. Res. 41 (17): 4201–4208.

16. Ház, A., Jablonský, M., Šurina, I., Kačík, F., Bubeníková, T., Ďurkovič J., 2019. Chemical composition and thermal behavior of kraft lignins. Forests 10 (6): 1–12.

17. Hu, C., Yang Y., Luo, J., Pan P., Tong, D., Li, G., 2011. Recent advances in the catalytic pyrolysis of biomass. Frontiers Chem. Eng. China 5 (2): 188–193.

18. Hu, S., Jess, A., Xu, M., 2007. Kinetic study of Chinese biomass slow pyrolysis: comparison of different kinetic models. Fuel 86 (17–18): 2778–2788.

19. Hussian, A.E.M., 2018. The role of microalgae in renewable energy production: challenges and opportunities. Marine Ecology - Biotic and Abiotic Interactions. InTech.

20. Imran, A., Bramer, E.A., Seshan, K., Brem,G., 2018. An overview of catalysts in biomass pyrolysis for production of biofuels. Biofuel Research Journal. Green Wave Publishing of Canada.

21. Kumar, S., Panda, A.K., Singh R.K., A review on tertiary recycling of high density

polyethylene to fuel. Resource. Conserv. Recycling 55(11), 893-910.

22. Lam, S.S., Mahari, W.A.W., Yong, S.O., Peng, W., Chong, C.T., Ma, N.Y., Chase, H.A., et al. 2019. Microwave vacuum pyrolysis of waste plastic and used cooking oil for simultaneous waste reduction and sustainable energy conversion: recovery of cleaner liquid fuel and techno-economic analysis. Renew. Sustain. Energy Rev. 115: 109359.

23. Li, K.Y., Huang, X., Fleischmann, C., Rein, G., Ji, J., 2014a. Pyrolysis of medium-density fiberboard: optimized search for kinetics scheme and parameters via a genetic algorithm driven by Kissinger's method. Energy Fuels 28 (9): 6130–6139.

24. Li, X., Li, J., Zhou, G., Feng, Y., Wang, Y., Yu, G., Deng, S., Huang, J., Wang, B., 2014b. Enhancing the production of renewable petrochemicals by co-feeding of biomass with plastics in catalytic fast pyrolysis with zsm-5 zeolites. Appl. Catalysis A: General 481: 173–182.

25. Li, X., 2014. Numerical Methods for Engineering Design and Optimization: Latin Hypercube Sampling (LHS).

26. Liew, J,X., Loy, A.C.M., Chin, B.L.F., AlNouss A., Shahbaz, M, Al-Ansari, T., Govindan, R., Chai, Y.H., 2021. Synergistic effects of catalytic co-pyrolysis of corn cob and hdpe waste mixtures using weight average global process. Renew. Energy (In Press). https://doi.org/10.1016/j.renene.2021.02.053.

27. Loy, A.C.M., Yusup, S., How, B.S., Yiin, C.L., Chin, B.L.F., Muhammad, M., Gwee, Y.L., 2019. Uncertainty estimation approach in catalytic fast pyrolysis of rice husk: thermal degradation, kinetic and thermodynamic analysis. Bioresourc. Technol. 294: 122089.

28. Manyà, J.J., Velo, E., Puigjaner L., 2003. Kinetics of biomass pyrolysis: a reformulated three-parallel-reactions model. Ind. Eng. Chem. Res. 42 (3): 434–441.

29. Mckay, M.D., Beckman, R.J., Conover, W.J., 2000. American society for quality a comparison of three methods for selecting values of input variables in the analysis of output from a computer code. Technometrics 42 (1): 55–61.

30. Mong, G.R., Ng, J.H., Chong, W.W.F., Ani, F.N., Lam, S.S., Chong, C.T., 2019. Kinetic study of horse manure through thermogravimetric analysis. Chem. Eng. Trans. 72: 241–246.

31. Ng, M.H., V. D., Sabu, T., Goh, K.L., 2019. Characteristics of Johorean Elaeis Guineensis oil palm kernel shells: elasticity, thermal stability, and biochemical composition. Biomass, Biopolymer-Based Materials, and Bioenergy: Construction, Biomedical, and Other Industrial Applications, 75–86.

32. Ng, Q.H., Chin, B.L.F., Yusup, S., Loy, C.M.A., Chong, K.Y.Y., 2018. Modeling of the

co-pyrolysis of rubber residual and HDPE waste using the distributed activation energy model (DAEM). Appl. Thermal Eng. 138: 336-345.

33. Ni X.,Wu, Z., Zhang, W., Lu, K., Ding, Y., Mao, S., 2020. Energy ulitization of building insulation waste expanded polystrene: pyrolysis kinetic estimation by a new comprehensive method. Polymers 12, 1744.

34. Olsson, A., Sandberg, G., Dahlblom, O., 2003. On latin hypercube sampling for structural reliability analysis. Structural Safety 25 (1): 47–68.

35. Önal, E., Başak, B.U.,Ayşe E.P., 2014. Bio-oil production via co-pyrolysis of almond shell as biomass and high density polyethylene. Energy Convers. Manage. 78: 704–710.

36. Phusunti, N., 2012. Pryolytic and kinetic study of chlorella vulgaris under isothermal and non-isothermal conditions. Aston University. Accessed 7 November 2020. https://publications.aston.ac.uk/id/eprint/19227/1/Studentthesis-2013.pdf.

37. Rotliwala, Y.C., Parikh, P.A., 2011. Thermal degradation of rice-bran with high density polyethylene: a kinetic study. Korean J. Chem. Eng 28 (3): 788–792.

38. Ryu, H.W., Kim, D.H., Jae, J., Lam, S.S., Park, E.D., Park, Y.K., 2020. Recent advances in catalytic co-pyrolysis of biomass and plastic waste for the production of petroleum-like hydrocarbons. Bioresourc. Technol. 310: 123473.

39. Ryu, H.W., Tsang Y.F., Lee H.W., Jae, J., Jung S.C., Lam, S.S., Park, E.D., Park Y.K., 2019. Catalytic co-pyrolysis of cellulose and linear low-density polyethylene over MgO-impregnated catalysts with different acid-vbse properties. Chem. Eng. 373: 375-381.

40. Wang, Q., Zhang, W., Sun, S., Wang, Z., Cui, D., 2020. Effect of CaO on pyrolysis products and reaction mechanisms of a corn stover. ACS Omega 5 (18): 10276–10287.

41. Xu, L., Jiang, Y., Wang L., 2017. Thermal decomposition of rape straw: pyrolysis modeling and kinetic study via particle swarm optimization. Energy Convers. Manage. 146: 124–133.

42. Xu, Y., Liu, Z., Peng, Y., You, T., Hu, X., 2017. Catalytic pyrolysis kinetics behavior of *Chlorella Pyrenoidosa* with thermal gravimetric analysis. J. Renew. Sustain. Energy 9 (6): 063105.

43. Yang, H., Yan, R., Chen, H., Lee D.H., Zheng, C., 2007. Characteristics of hemicellulose, cellulose and lignin pyrolysis. Fuel 86 (12–13): 1781–1788.

44. Zullaikah, S., Utomo, A.T., Yasmin, M., Ong, L.K., Ju, Y.H., 2019. Ecofuel Conversion Technology of Inedible Lipid Feedstocks to Renewable Fuel. in Advances in Eco-Fuels for a Sustainable Environment, 237–276. Elsevier.

Figure

Click here to access/download;Figure;Figures_BITEv1.docx

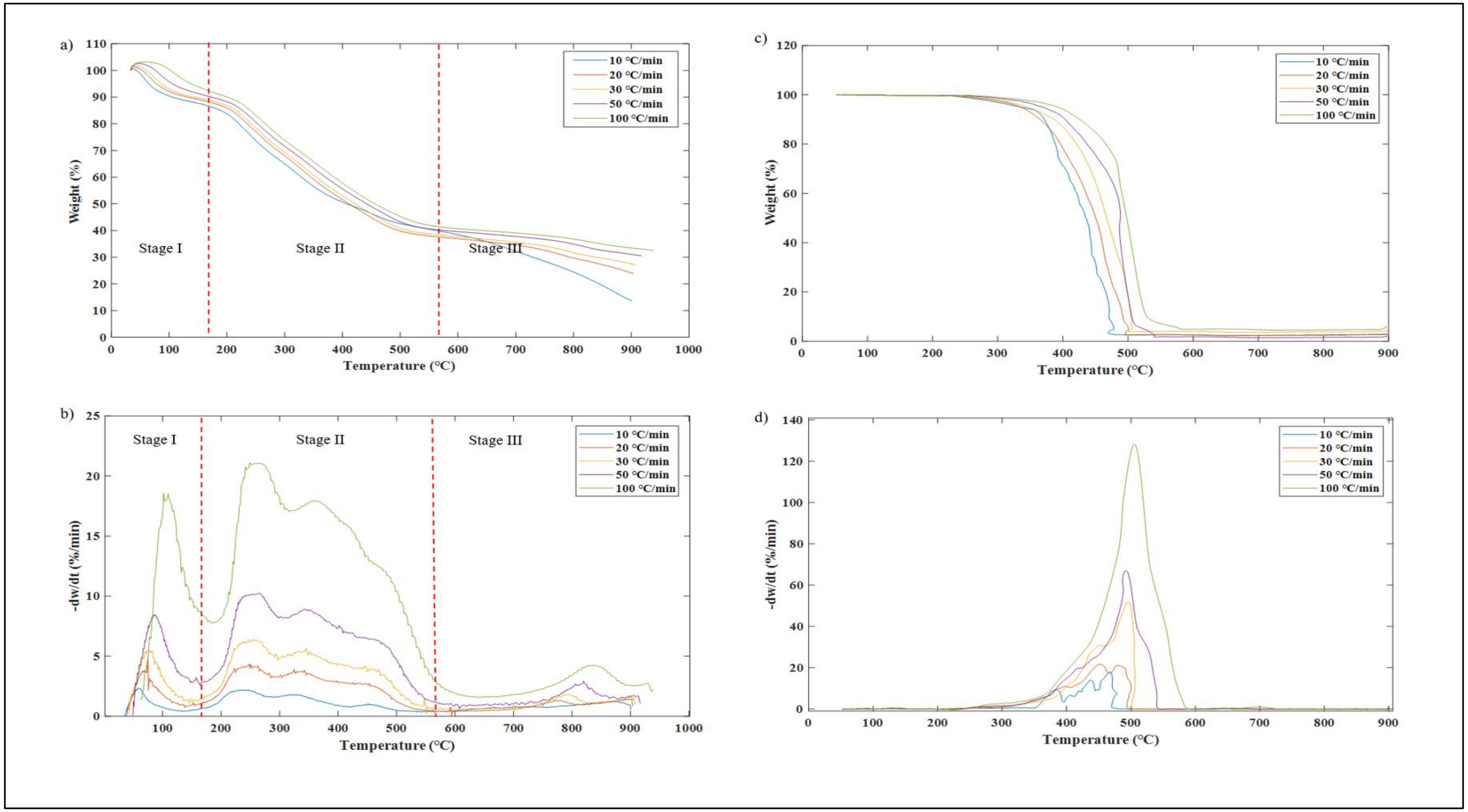

Fig. 1. (a) TG curves for pure microalgae *Chlorella vulgaris*, (b) DTG curves for pure microalgae *Chlorella vulgaris*, (c) TG curves for pure HDPE, and (d) DTG curves for pure HDPE.

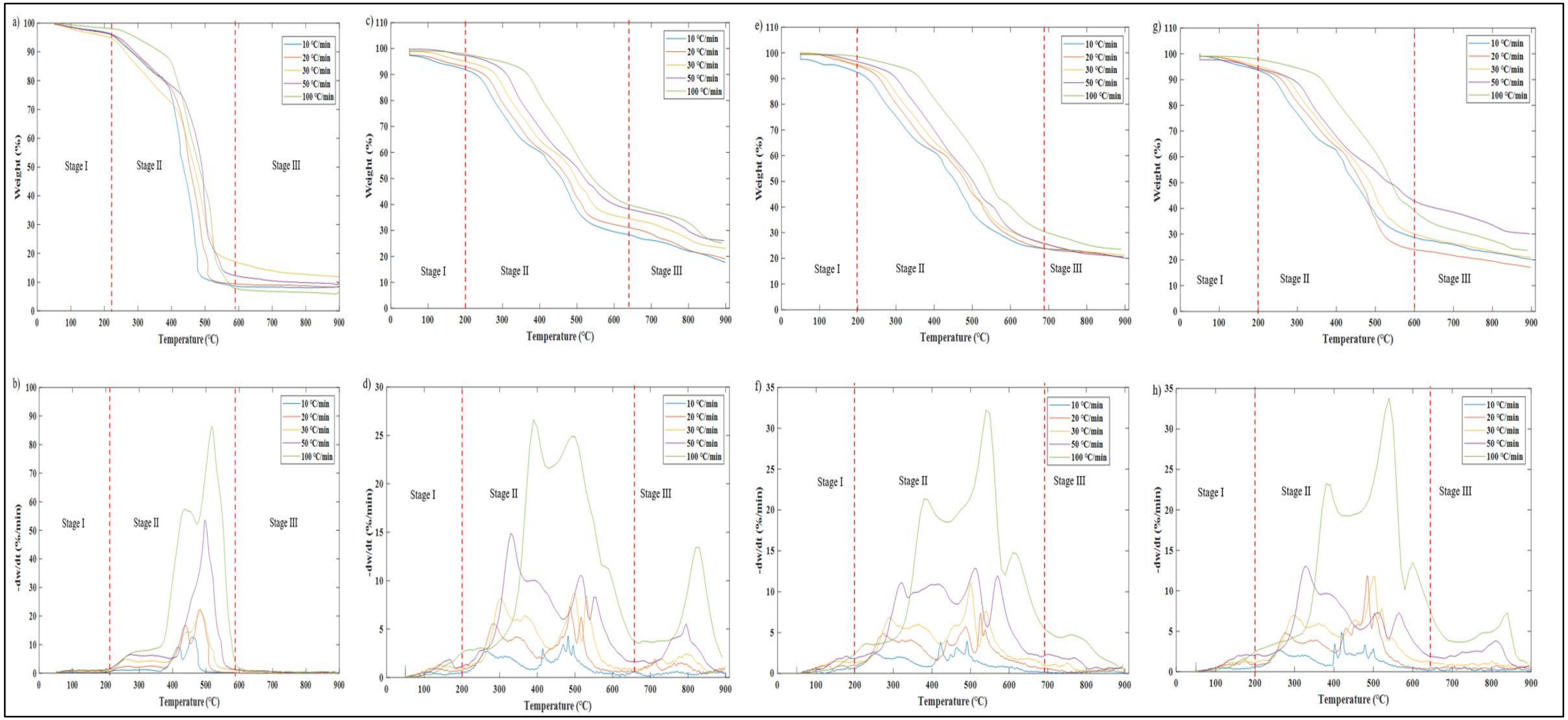

Fig. 2. (a) TG curves for binary mixture of microalgae *Chlorella vulgaris* and HDPE, (b) DTG curves for binary mixture of microalgae *Chlorella vulgaris* and HDPE, (c) TG curves for binary mixture of pure microalgae *Chlorella vulgaris* and HDPE mixture with LS catalyst, (d) DTG curves for binary mixture of pure microalgae *Chlorella vulgaris* and HDPE mixture with LS catalyst, (e) TG curves for binary mixture of pure microalgae *Chlorella vulgaris* and HDPE mixture with HZSM-5 catalyst, (f) DTG curves for binary mixture of pure microalgae *Chlorella vulgaris* and HDPE mixture with HZSM-5 catalyst, (g) TG curves for binary mixture of pure microalgae *Chlorella vulgaris* and HDPE mixture with LS/HZSM-5 catalyst, and (h) DTG curves for binary mixture of pure microalgae *Chlorella vulgaris* and HDPE mixture with LS/HZSM-5 catalyst.

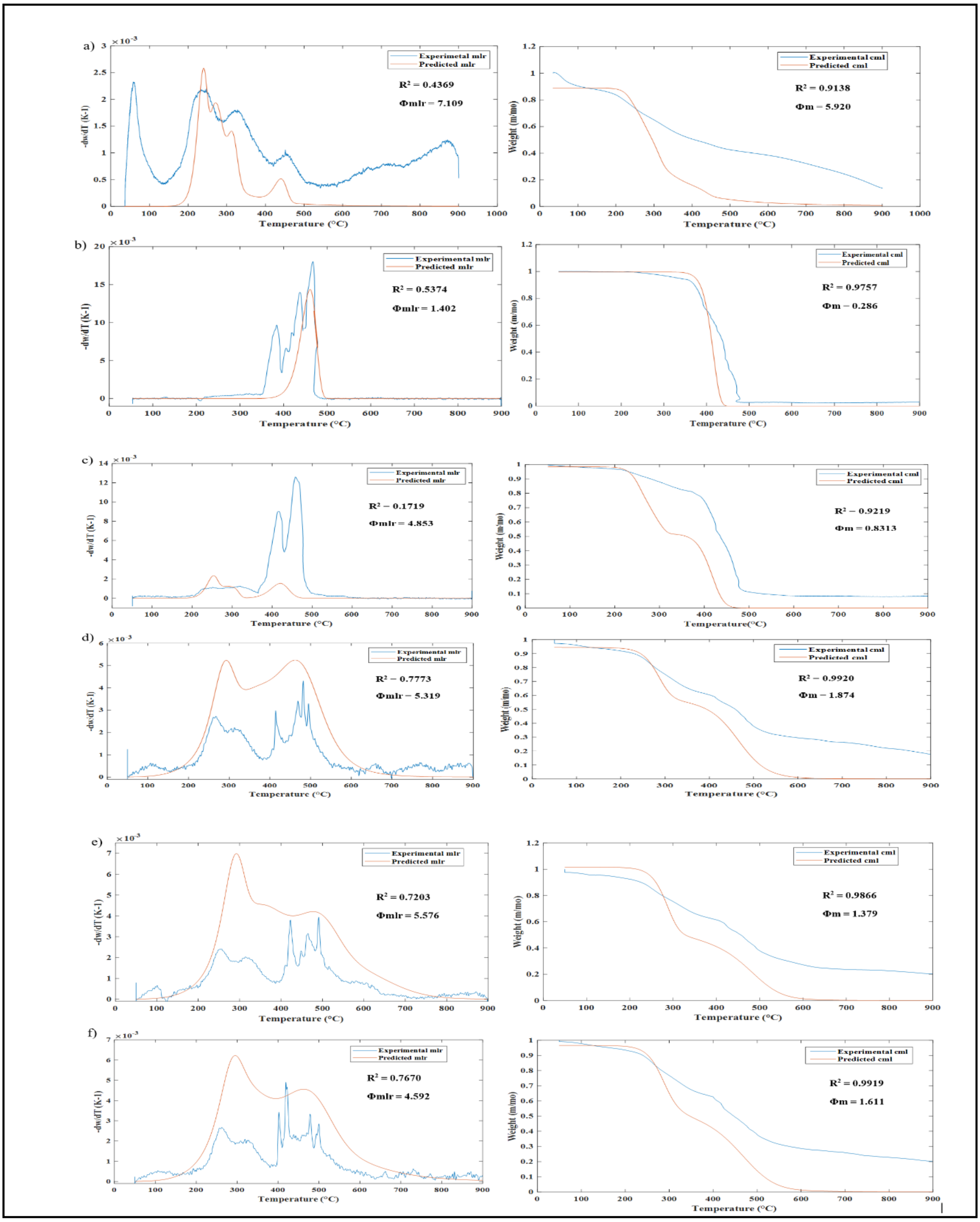

Fig. 3. Predicted and experimental mlr and cml graphs for (a) pure microalgae *Chlorella vulgaris*, (b) pure HDPE, (c) microalgae *Chlorella vulgaris* and HDPE mixture, (d) microalgae *Chlorella vulgaris* and HDPE mixture with LS catalyst, (e) microalgae *Chlorella vulgaris* and HDPE mixture with HZSM-5 catalyst, and (f) microalgae *Chlorella vulgaris* and HDPE mixture with LS/HZSM-5 catalyst.

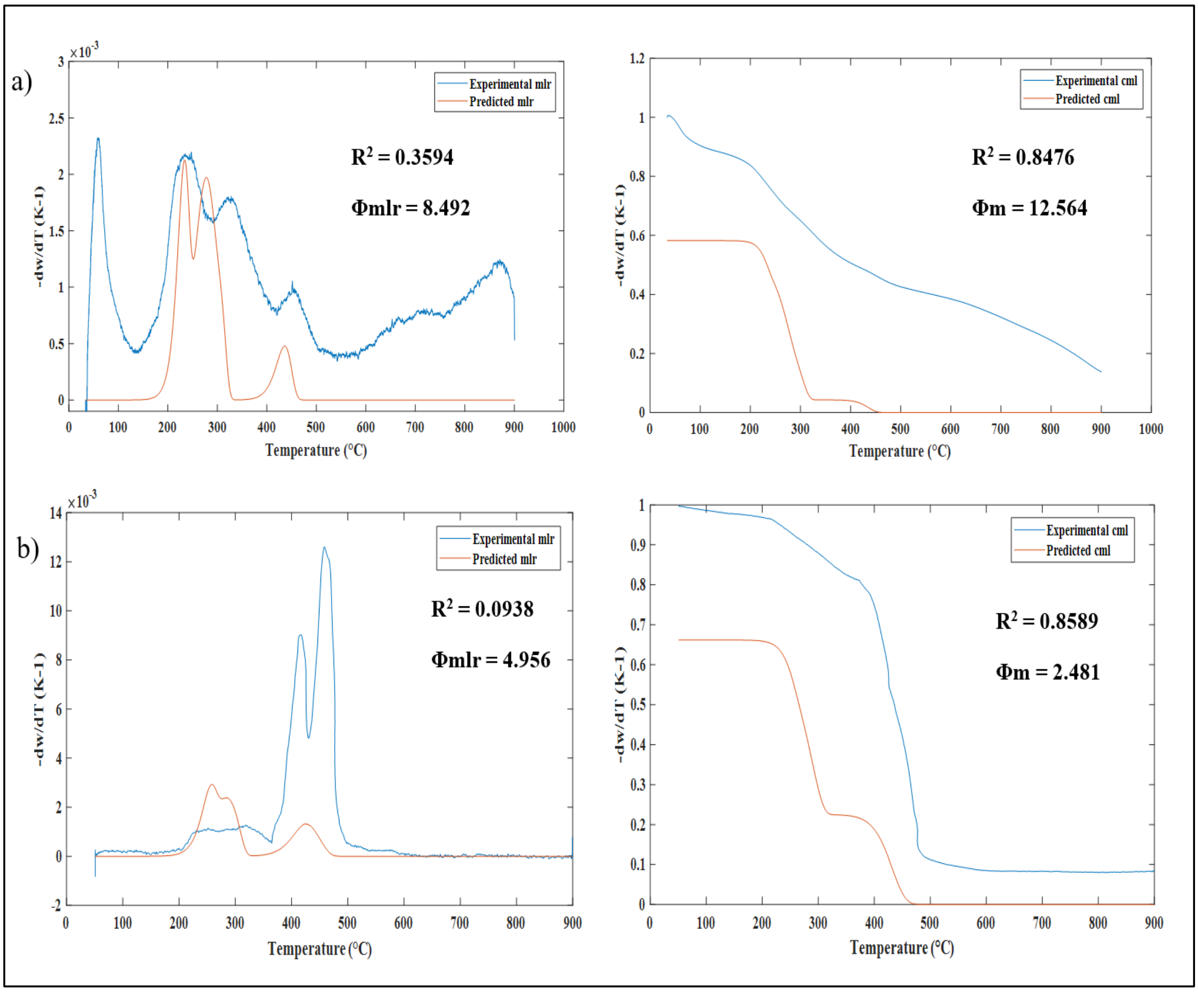

Fig. 4. Predicted and experimental mlr and cml graphs for (a) pure microalgae *Chlorella vulgaris* before optimization, and (b) microalgae *Chlorella vulgaris* and HDPE mixture before optimization.

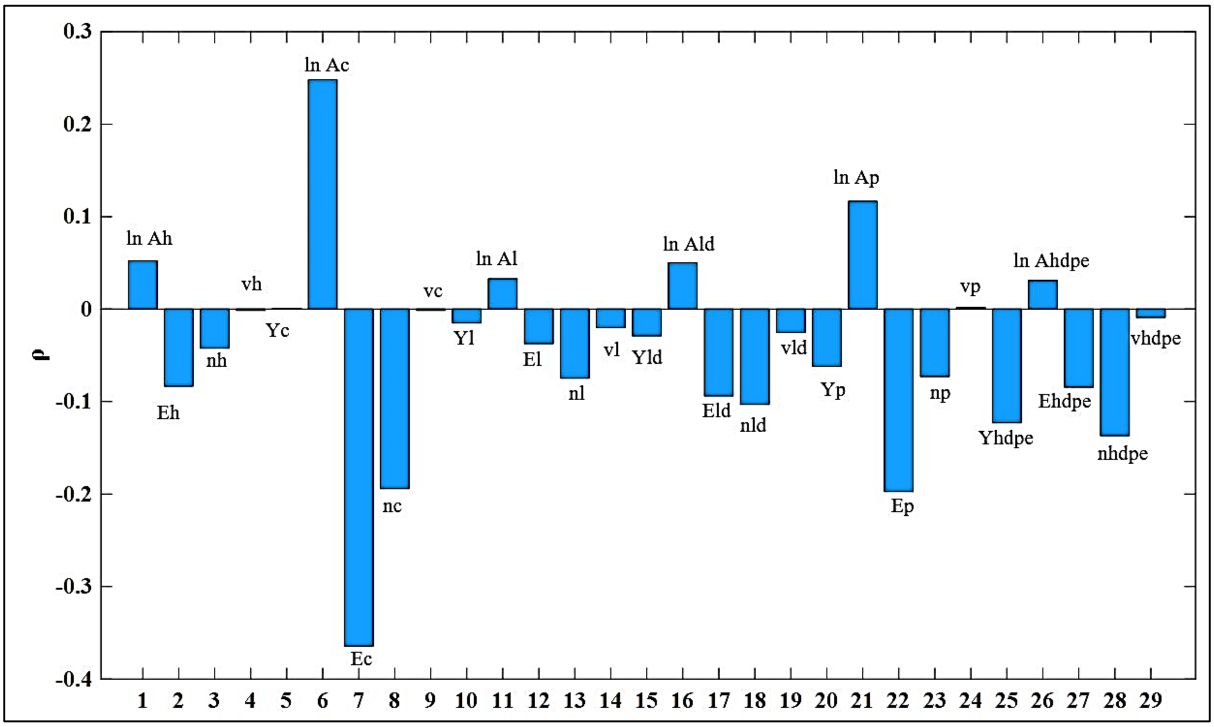

Fig. 5. Sensitivity analysis of the parameters used to obtain the predicted thermogravimetric results.

Table 1: Initial, final and maximum degradation temperature of the main decomposition stage, mass loss, amount of residue, and maximum degradation rate values of the pyrolysis samples.

Sample	Heating Rate (ºC/min)	Second Stage					Third Stage Residue (%)
		$T_{initial}$ (ºC)	T_{final} (ºC)	T_m (ºC)	Mass Loss (%)	DTG max (%/min)	
Microalgae *Chlorella vulgaris*	10	136.7	542.5	247.8	47.530	2.196	13.760 ± 0.121
	20	138.1	556.8	250.7	51.880	4.330	23.910 ± 0.181
	30	145.2	578.6	255.2	51.800	6.370	27.140 ± 0.052
	50	147.5	579.6	257.5	51.550	10.110	30.540 ± 0.221
	100	177.0	619.4	267.1	51.380	21.050	32.580 ± 0.125
HDPE	10	228.3	480.3	467.5	96.830	18.030	2.670 ± 0.157
	20	220.1	500.6	452.2	97.182	21.640	2.578 ± 0.218
	30	236.6	505.8	496.3	95.763	52.020	3.907 ± 0.193
	50	245.8	547.5	492.3	97.982	66.870	1.778 ± 0.274
	100	253.8	592.0	505.8	94.914	128.200	4.856 ± 0.126
Microalgae *Chlorella vulgaris* + HDPE	10	364.8	515.8	458.3	71.400	12.610	8.436 ± 0.167
	20	373.4	558.5	482.7	71.495	22.260	8.626 ± 0.325
	30	376.8	578.9	485.3	56.680	21.870	12.020 ± 0.354
	50	395.4	594.8	497.1	66.540	53.570	9.546 ± 0.224
	100	362.1	605.7	517.9	82.943	86.390	6.429 ± 0.219
Microalgae *Chlorella vulgaris* + HDPE + LS	10	157.0	596.0	482.0	63.930	4.320	17.670 ± 0.183
	20	176.0	616.0	486.0	62.070	7.310	19.020 ± 0.120
	30	179.0	638.0	497.0	61.150	8.700	22.980 ± 0.188
	50	200.0	680.0	330.0	60.770	14.870	26.090 ± 0.195
	100	270.0	710.0	390.0	58.630	26.660	25.150 ± 0.100
Microalgae *Chlorella vulgaris* + HDPE+ HZSM-5	10	135.0	651.0	491.0	70.780	3.940	20.290 ± 0.123
	20	190.0	658.0	526.0	70.550	7.390	20.071 ± 0.119
	30	203.0	668.0	500.0	68.870	11.060	21.072 ± 0.183
	50	210.0	685.0	510.0	70.150	12.840	20.560 ± 0.129
	100	250.0	720.0	540.0	67.970	32.250	23.530 ± 0.155
Microalgae *Chlorella vulgaris* + HDPE + LS/HZSM-5	10	159.0	623.0	419.0	67.400	4.900	20.180 ± 0.123
	20	206.0	624.0	484.0	70.210	11.870	17.070 ± 0.119
	30	223.0	629.0	500.0	65.460	11.760	20.940 ± 0.088
	50	225.0	680.0	330.0	54.190	13.030	30.121 ± 0.429
	100	280.0	710.0	540.0	64.020	33.800	23.660 ± 0.156

Table 2: Calculated kinetic parameters for all samples.

Sample	Component	E_A (kJ/mol)	A (s^{-1})	ln A [ln(s^{-1})]	R^2
Microalgae *Chlorella vulgaris*	Cellulose	183.66	8.85×10^{16}	39.02	0.8777
	Lipid	233.66	2.29×10^{18}	42.28	0.8767
	Lignin	269.29	3.33×10^{17}	40.35	0.8074
HDPE	-	255.52	9.29×10^{15}	36.77	0.8789
Microalgae *Chlorella vulgaris* + HDPE	Cellulose	175.87	2.80×10^{15}	35.58	0.9393
	Lipid	210.34	4.05×10^{16}	38.24	0.8313
	Lignin	204.05	1.99×10^{13}	30.62	0.9039
	HDPE	194.96	4.85×10^{11}	26.91	0.9806
Microalgae *Chlorella vulgaris* + HDPE + LS	Cellulose	42.65	5.09×10^{1}	3.93	0.9522
	Lipid	38.15	6.39	1.86	0.9091
	Lignin	154.47	4.47×10^{8}	19.92	0.9957
	HDPE	128.87	2.69×10^{6}	14.80	0.9875
Microalgae *Chlorella vulgaris* + HDPE + HZSM-5	Cellulose	41.62	4.81×10^{1}	3.87	0.9331
	Lipid	74.50	1.42×10^{4}	9.56	0.9953
	Lignin	76.65	1.46×10^{3}	7.29	0.8603
	HDPE	95.43	1.20×10^{4}	9.39	0.9954
Microalgae *Chlorella vulgaris* + HDPE + LS/HZSM-5	Cellulose	43.48	6.69×10^{1}	4.20	0.9521
	Lipid	72.34	9.25×10^{3}	9.13	0.9371
	Lignin	72.74	7.65×10^{2}	6.64	0.8552
	HDPE	83.20	2.05×10^{3}	7.62	0.9746

Table 3: Search range and optimized values by PSO for microalgae *Chlorella vulgaris* and HDPE mixture with LS/HZSM-5 catalyst.

Components	**Parameters**	**Initial Values**	**Search Range**		**Optimized Values**
			Lower	**Upper**	
Hemicellulose	Yh	0.03	-	-	0.05
	ln Ah [ln (s−1)]	21.31	10.66	31.97	21.44
	Eh (kJ/mol)	117.12	58.56	175.68	117.31
	vh	0.23	0.12	0.35	0.18
	nh	1.00	0.00	5.00	1.18
Cellulose	Yc	0.07	0.03	0.10	0.06
	ln Ac [ln (s−1)]	4.20	2.10	6.30	5.20
	Ec (kJ/mol)	43.48	21.74	65.21	43.72
	vc	0.06	0.03	0.09	0.07
	nc	1.00	0.00	5.00	1.52
Lignin	Yl	0.06	0.03	0.09	0.05
	ln Al [ln (s−1)]	6.64	3.32	9.96	6.85
	El (kJ/mol)	72.74	36.37	109.10	72.99
	vl	0.46	0.23	0.69	0.57
	nl	1.00	0.00	5.00	1.81
Lipid	Yld	0.21	0.11	0.32	0.21
	ln Ald [ln (s−1)]	9.13	4.57	13.70	9.88
	Eld (kJ/mol)	72.34	36.17	108.50	72.28
	vld	0.46	0.00	0.92	0.86
	nld	1.00	0.00	5.00	1.15
Protein	Yp	0.42	0.21	0.64	0.43
	ln Ap [ln (s−1)]	19.31	9.65	28.96	19.75
	Ep (kJ/mol)	118.13	59.07	177.20	118.64
	vp	0.46	0.00	0.92	0.37
	np	1.00	0.00	5.00	1.46
HDPE	Yhdpe	0.20	0.10	0.50	0.19
	ln Ahdpe [ln (s−1)]	7.62	3.81	11.44	7.66
	Ehdpe (kJ/mol)	83.20	41.60	124.80	83.60
	vhdpe	0.04	0.00	0.09	0.07
	nhdpe	1.00	0.00	5.00	1.21

Table 4: Optimized kinetic parameters.

Sample	**Components**	***A*** **(s^{-1})**	**E_A (kJ mol^{-1})**	***n***
Microalgae *Chlorella vulgaris*	H	1.94×10^{9}	117.27	0.85
	C	1.04×10^{17}	183.86	0.96
	L	2.28×10^{17}	269.65	1.09
	Ld	2.39×10^{18}	233.55	1.33
	P	1.45×10^{8}	118.66	4.75
	Average	$\mathbf{5.44 \times 10^{17}}$	**184.60**	**1.80**
HDPE	-	5.01×10^{14}	253.79	1.00
Microalgae *Chlorella vulgaris* + HDPE	H	2.55×10^{9}	117.69	1.44
	C	2.90×10^{15}	175.92	1.04
	L	2.86×10^{13}	204.46	1.18
	Ld	4.12×10^{16}	210.93	1.04
	P	3.17×10^{8}	118.00	1.26
	HDPE	4.98×10^{11}	195.14	1.30
	Average	$\mathbf{6.38 \times 10^{15}}$	**170.36**	**1.21**
Microalgae *Chlorella vulgaris* + HDPE + LS	H	2.52×10^{9}	117.83	1.23
	C	6.15×10^{1}	42.66	1.40
	L	5.99×10^{8}	154.60	2.15
	Ld	8.47×10^{0}	38.52	1.23
	P	3.85×10^{8}	118.21	1.27
	HDPE	3.55×10^{6}	128.69	1.69
	Average	$\mathbf{5.85 \times 10^{8}}$	**100.09**	**1.50**
Microalgae *Chlorella vulgaris* + HDPE + HZSM-5	H	2.08×10^{9}	117.39	1.01
	C	6.14×10^{1}	41.59	1.13
	L	1.47×10^{3}	66.35	1.31
	Ld	1.50×10^{4}	74.80	1.44
	P	3.74×10^{8}	118.16	1.17
	HDPE	1.23×10^{4}	95.62	1.25
	Average	$\mathbf{4.08 \times 10^{8}}$	**87.42**	**1.22**
Microalgae *Chlorella vulgaris* + HDPE + LS/HZSM-5	H	2.04×10^{9}	117.31	1.18
	C	1.82×10^{2}	43.72	1.52
	L	9.40×10^{2}	72.99	1.81
	Ld	1.96×10^{4}	72.28	1.15
	P	3.77×10^{8}	118.64	1.46
	HDPE	2.12×10^{3}	83.60	1.21
	Average	$\mathbf{4.03 \times 10^{8}}$	**83.59**	**1.39**

Table 5: Thermodynamic parameters for the pyrolysis of the samples.

Sample	Heating Rate (°C/min)	T_m (°C)	T_m (K)	ΔH (J/mol)	ΔG (J/mol)	ΔS (J/mol.K)
Microalgae *Chlorella vulgaris*	10	247.8	520.95	1.80×10^5	1.38×10^5	81.67
	20	250.7	523.85	1.80×10^5	1.37×10^5	81.62
	30	255.2	528.35	1.80×10^5	1.37×10^5	81.55
	50	257.5	530.65	1.80×10^5	1.37×10^5	81.52
	100	267.1	540.25	1.80×10^5	1.36×10^5	81.37
HDPE	10	467.5	740.65	2.48×10^5	2.32×10^5	20.63
	20	452.2	725.35	2.48×10^5	2.33×10^5	20.80
	30	496.3	769.45	2.47×10^5	2.32×10^5	20.31
	50	492.3	765.45	2.47×10^5	2.32×10^5	20.36
	100	505.8	778.95	2.47×10^5	2.32×10^5	20.21
Microalgae *Chlorella vulgaris* + HDPE	10	458.3	731.45	1.64×10^5	1.34×10^5	41.88
	20	482.7	755.85	1.64×10^5	1.33×10^5	41.61
	30	485.3	758.45	1.64×10^5	1.33×10^5	41.58
	50	497.1	770.25	1.64×10^5	1.32×10^5	41.45
	100	517.9	791.05	1.64×10^5	1.67×10^5	-4.67
Microalgae *Chlorella vulgaris* + HDPE + LS	10	482	755.15	9.38×10^4	1.64×10^5	-93.11
	20	486	759.15	9.38×10^4	1.64×10^5	-93.16
	30	497	770.15	9.37×10^4	1.66×10^5	-93.28
	50	330	603.15	9.51×10^4	1.50×10^5	-91.25
	100	390	663.15	9.46×10^4	1.56×10^5	-92.03
Microalgae *Chlorella vulgaris* + HDPE + HZSM-5	10	491	764.15	8.11×10^4	1.55×10^5	-96.20
	20	526	799.15	8.08×10^4	1.58×10^5	-96.58
	30	500	773.15	8.10×10^4	1.55×10^5	-96.30
	50	510	783.15	8.09×10^4	1.56×10^5	-96.41
	100	540	813.15	8.07×10^4	1.59×10^5	-96.72
Microalgae *Chlorella vulgaris* + HDPE + LS/HZSM-5	10	419	692.15	7.78×10^4	1.44×10^5	-95.49
	20	484	757.15	7.73×10^4	1.50×10^5	-96.24
	30	500	773.15	7.72×10^4	1.52×10^5	-96.41
	50	330	603.15	7.86×10^4	1.35×10^5	-94.35
	100	540	813.15	7.68×10^4	1.56×10^5	-96.83

Table 6: LHS samples and rank transformed parameters.

															LHS Sampling															
	lnAh	**Eh**	**nh**	**vh**	**Yc**	**lnAc**	**Ec**	**nc**	**vc**	**Yl**	**lnAl**	**El**	**nl**	**vl**	**Yld**	**lnAld**	**Eld**	**nld**	**vld**	**Yp**	**lnAp**	**Ep**	**np**	**vp**	**Yhdpe**	**lnAhdpe**	**Ehdpe**	**nhdpe**	**vhdpe**	**phi**
1	13.36	166.34	1.70	0.26	0.07	9.20	61.93	0.94	0.05	0.03	4.07	76.48	0.33	0.46	0.12	8.72	102.15	2.98	0.43	0.32	11.20	118.49	1.57	0.89	0.26	10.17	68.72	0.29	0.05	62.87
2	17.47	135.12	2.72	0.21	0.09	10.68	39.60	3.49	0.04	0.06	4.43	64.81	3.57	0.29	0.19	10.56	65.92	2.86	0.54	0.26	16.77	123.60	0.25	0.20	0.39	9.81	104.27	1.87	0.01	45.31
3	28.81	123.21	2.61	0.28	0.07	4.99	27.49	0.32	0.08	0.08	8.18	94.51	0.21	0.52	0.20	6.56	71.05	1.19	0.51	0.38	10.11	163.64	1.26	0.79	0.10	8.12	54.86	4.12	0.03	114.04
4	20.71	146.18	0.71	0.30	0.05	9.32	25.58	3.69	0.05	0.03	5.90	58.49	0.13	0.24	0.31	6.85	68.47	1.66	0.33	0.40	25.03	133.91	3.24	0.44	0.41	10.89	120.45	3.21	0.01	854.13
5	20.71	76.59	1.54	0.17	0.09	7.97	24.64	2.62	0.04	0.09	3.54	70.94	4.78	0.44	0.27	7.00	70.15	2.37	0.49	0.45	17.12	138.49	1.96	0.29	0.45	6.77	122.11	0.91	0.00	625.92
6	23.92	109.93	0.80	0.22	0.10	7.40	61.80	4.11	0.06	0.09	4.74	63.34	1.41	0.68	0.25	9.30	50.46	3.77	0.62	0.45	28.77	129.21	3.60	0.69	0.18	10.24	91.86	4.54	0.09	15.39
7	30.92	80.66	2.31	0.30	0.04	10.51	50.10	4.08	0.04	0.04	8.38	80.33	2.60	0.30	0.22	9.77	107.75	2.51	0.04	0.48	26.38	92.10	0.12	0.35	0.19	10.49	94.72	0.10	0.07	1449.76
8	14.83	166.57	4.34	0.28	0.06	10.85	56.87	2.09	0.06	0.05	9.40	84.45	3.55	0.48	0.20	5.32	94.05	1.02	0.09	0.42	12.17	66.92	3.87	0.55	0.11	6.25	123.02	0.41	0.07	14.93
9	29.34	82.60	4.68	0.26	0.08	8.15	29.26	0.27	0.06	0.06	8.06	102.30	2.58	0.43	0.24	9.39	77.96	3.89	0.87	0.34	25.21	144.79	4.81	0.44	0.33	7.65	116.87	1.62	0.06	470.71
10	29.21	84.34	0.26	0.31	0.09	10.68	57.73	4.96	0.07	0.08	4.99	71.65	3.77	0.65	0.26	9.81	36.90	3.99	0.18	0.58	13.17	171.25	1.19	0.45	0.45	7.94	59.19	1.90	0.06	65.45
11	16.73	166.13	1.82	0.18	0.05	8.25	27.61	3.43	0.04	0.05	3.51	53.56	4.09	0.42	0.31	8.68	45.84	3.36	0.84	0.26	28.09	104.65	3.56	0.47	0.19	6.71	89.19	3.74	0.05	151.16
12	13.37	140.20	2.12	0.20	0.07	5.97	54.65	3.79	0.05	0.08	5.59	57.87	4.64	0.37	0.25	7.88	57.65	2.80	0.11	0.27	23.89	102.66	3.08	0.82	0.19	4.12	70.50	1.13	0.02	18.17
13	28.55	150.23	2.90	0.19	0.06	6.29	44.81	4.04	0.08	0.06	9.20	108.72	1.13	0.43	0.22	5.33	55.63	4.93	0.44	0.22	26.37	134.46	1.95	0.42	0.35	7.93	92.25	4.71	0.07	9.60
14	22.01	78.46	1.51	0.17	0.09	2.70	37.40	1.81	0.05	0.06	3.81	84.23	4.73	0.30	0.22	4.87	55.51	2.02	0.54	0.39	11.94	155.95	2.72	0.28	0.47	9.45	119.36	2.61	0.03	9.03
15	14.70	102.27	1.52	0.16	0.04	11.03	43.79	0.26	0.08	0.03	6.28	98.24	3.92	0.41	0.24	6.39	72.44	3.95	0.83	0.23	19.49	102.03	3.96	0.21	0.22	8.85	98.39	0.22	0.03	133.23
16	15.61	133.82	1.73	0.20	0.03	3.12	30.29	3.33	0.06	0.08	7.80	96.63	0.29	0.50	0.22	12.29	81.60	2.50	0.69	0.36	23.78	171.76	3.09	0.64	0.13	4.71	53.75	0.25	0.09	105.34
17	29.33	160.19	3.01	0.32	0.05	9.14	58.84	4.34	0.05	0.07	4.27	38.85	0.49	0.39	0.24	11.87	39.36	4.80	0.78	0.39	21.82	101.36	3.33	0.32	0.46	5.05	66.08	4.33	0.07	24.82
18	27.13	135.00	0.05	0.27	0.08	9.77	42.38	4.68	0.05	0.06	4.90	61.41	1.77	0.59	0.13	7.01	51.51	1.77	0.36	0.30	20.18	61.29	4.93	0.47	0.49	5.56	118.68	0.56	0.06	116.08
19	10.98	92.39	3.18	0.21	0.06	8.15	60.67	3.32	0.06	0.05	6.91	98.52	0.64	0.57	0.29	6.56	51.87	1.52	0.14	0.49	16.82	98.89	2.59	0.28	0.26	5.30	122.02	0.38	0.09	8.37
20	27.69	68.79	4.20	0.24	0.08	4.11	60.25	2.85	0.07	0.06	9.88	55.22	1.28	0.48	0.29	8.86	52.88	4.46	0.48	0.57	14.20	155.71	3.03	0.16	0.21	4.10	65.03	4.07	0.03	10.40
															Rank Transformation															
	lnAh	**Eh**	**nh**	**vh**	**Yc**	**lnAc**	**Ec**	**nc**	**vc**	**Yl**	**lnAl**	**El**	**nl**	**vl**	**Yld**	**lnAld**	**Eld**	**nld**	**vld**	**Yp**	**lnAp**	**Ep**	**np**	**vp**	**Yhdpe**	**lnAhdpe**	**Ehdpe**	**nhdpe**	**vhdpe**	**phi**
1	2531	18406	6787	12493	10489	13507	18491	3760	6826	1650	2274	11031	1318	10073	762	9089	18246	11927	9321	4932	1604	10062	6289	19379	7754	16661	6520	1156	10759	11571
2	6396	13074	10892	7922	18261	16329	8217	13963	2037	8710	3353	7822	14268	2400	7493	13115	8228	11444	11670	2376	7371	10927	1011	4334	14649	15728	15066	7467	1501	10611
3	17033	11040	10426	14296	10126	5505	2646	1289	17293	15859	14633	15989	860	12788	8816	4352	9644	4757	11119	7707	472	17706	5040	17268	198	11301	3189	16476	6575	12998
4	9431	14963	2850	15732	4369	13742	1766	14749	6244	357	7769	6083	512	368	19070	4989	8931	6638	7178	8814	15932	12672	12970	9520	15711	18571	18955	12839	1190	16315
5	9433	3079	6160	4132	15955	11175	1337	10471	2293	18970	655	9506	19117	9038	15162	5329	9396	9480	10640	10933	7734	13447	7827	6253	17541	7771	19353	3624	531	15897
6	12450	8773	3182	8293	19258	10092	18430	16441	8897	19022	4282	7418	5638	19559	13026	10353	3952	15061	13539	10971	19807	11877	14399	15027	3890	16846	12082	18171	19111	4711
7	19016	3775	9227	15934	4145	16012	13048	16337	4359	3133	15251	12090	10418	3241	10399	11388	19792	10050	797	12670	17333	5594	462	7684	4272	17517	12769	414	15628	16910
8	3913	18445	17373	13659	9258	16656	16163	8370	9708	5739	18325	13223	14192	10711	9003	1633	16004	4081	1899	9710	2612	1331	15473	11863	718	6397	19572	1629	15898	4476
9	17528	4106	18736	11948	15583	11510	3461	1071	10780	10041	14279	18130	10318	8495	12013	10561	11555	15575	18926	6078	16112	14515	19244	9560	11303	10059	18095	6466	13314	15499
10	17407	4403	1032	16339	16874	16325	16559	19822	13259	16220	5016	9702	15080	18069	14435	11471	203	15961	3900	17087	3642	18994	4773	9699	17443	10830	4230	7589	13949	11687
11	5696	18369	7284	5242	7025	11707	2699	13732	2652	5915	585	4727	16367	8315	18724	9012	2674	13431	18231	2492	19100	7719	14253	10118	4354	7599	11441	14975	10210	13617
12	2540	13942	8471	7075	10499	7370	15140	15154	5382	18200	6844	5914	18545	6133	13107	7254	5940	11190	2284	2995	14750	7381	12306	17799	4261	825	6948	4508	4255	5921
13	16794	15654	11594	6234	7790	7972	10617	16165	15014	11329	17697	19895	4508	8662	10008	1676	5381	19734	9624	234	17313	12765	7820	9030	12345	10789	12176	18844	15814	1601
14	10649	3398	6039	4481	16087	1146	7205	7223	5183	10969	1478	13162	18915	2878	10351	662	5349	8075	11777	8533	2368	16403	10891	6125	18501	14778	18694	10437	7445	1292
15	3796	7464	6100	3372	2081	17001	10147	1021	17519	453	8918	17015	15700	7820	12639	3988	10030	15811	18078	784	10191	7275	15822	4552	6047	13219	13651	893	6568	13347
16	4646	12852	6903	7243	1023	1949	3935	13328	9521	16231	13506	16571	1165	11578	10943	16921	12561	9996	15092	7033	14640	19080	12378	13939	1564	2360	2922	1005	19822	12834
17	17522	17356	12022	17009	6063	13388	17068	17375	6229	14975	2876	683	1968	7165	12427	15986	883	19217	16968	8559	12609	7161	13306	6861	18094	3257	5885	17319	14078	7959
18	15458	13053	182	12755	13692	14599	9496	18714	5477	9803	4752	6887	7072	15468	1841	5341	4243	7099	7820	4295	10907	377	19724	10223	19624	4590	18530	2247	13637	13027
19	300	5777	12738	7485	9290	11521	17910	13265	11635	6209	10824	17091	2576	14601	17231	4364	4342	6082	2965	13191	7431	6743	10346	6127	7956	3904	19333	1532	19021	983
20	15980	1747	16807	10312	14120	3828	17718	11403	14950	8554	19761	5183	5121	10667	16963	9390	4622	17852	10506	16655	4718	16363	12111	3553	5482	762	5632	16271	7193	2017

CRediT authorship contribution statement

Mahrima Majid – Writing – original draft, Formal analysis, Investigation, Software

Bridgid Lai Fui Chin – Supervision, Validation, Writing – review & editing, Project administration, Visualization

Zeinab Abbas Jawad – Writing – review & editing

Yee Ho Chai – Data curation

Man Kee Lam – Resources

Suzana Yusup – Resources

Kin Wai Cheah – Writing – review & editing

Declarations of interest: None